A Reciprocal Space Approach to the Orbitals of Truncated Crystals[1]

Ralph A. Wheeler,*,† Lucjan Piela,§ and Roald Hoffmann*

Contribution from the Department of Chemistry and Materials Science Center, Cornell University, Ithaca, New York 14853. *Received January 25, 1988*

Abstract: Large clusters and small crystallites are a form of matter intermediate between discrete molecules and infinite solids. At the same time as they are structurally intriguing, they are difficult to treat by using conventional orbital methods. A linear combination of crystal orbitals (LCCO) method is described for calculating the orbitals of large, finite systems such as clusters, crystallites, or thin films from a band calculation on the corresponding infinite solid. Our analysis breaks the problem into two parts: (1) choosing k points where orbitals of the solid resemble cluster MO's and (2) performing a perturbation calculation to include the effects of truncating the crystal and of adding the end atoms omitted from the band calculation. The reciprocal space of the finite crystal and its relation to the reciprocal lattice of the infinite solid provide a fundamental connection between cluster MO's and crystal orbitals of the solid. Wannier functions localized within a large unit cell corresponding to the cluster make the connection explicit and guide the choice of k points for the band calculation. In the final step, the perturbation calculation is accomplished by using a matrix diagonalization algorithm introduced by Davidson to solve the CI problem for small molecules. The LCCO method is illustrated for hydrocarbon polyenes and transition-metal chains related to $[Rh(CN(CH_2)_3NC)_2]_4Cl^{5+}$. Both the delocalized levels and the orbitals localized near the edges of the clusters are reliably reproduced. For the Rh_4 chain we find that the central Rh–Rh bond can be shortened by making terminal ligands more electronegative or lengthened by less electronegative capping groups. Preferred cluster electron counts can be found by locating low densities of states in the corresponding solid. For the Rh_n oligomers, they appear within the steep z^2 band of the infinite polymer—at electron counts near d^7–d^8. The HOMO for long Rh_n oligomers with d^7–d^8 electron counts will therefore have metal z^2 character and fall in the energy range spanned by the z^2 band of the infinite polymer. Although the method is illustrated with extended Hückel calculations for large clusters, the LCCO approach is general and can be used with any orbital method. The approach is also valid for other systems perturbed from perfect translational symmetry, such as surfaces, interfaces, and defects.

The study of unusual materials with novel properties represents a strong and growing current in modern chemistry. Witness, for example, the discovery of heavy fermion superconductors,[2] organic ferromagnets,[3] and high T_c oxide superconductors.[4] Excitement over these and other recent advances has increased the trickle of new solid-state compounds to a flood. And traditional solid-state chemists are not alone in their search for intriguing new materials. Molecular chemists have been swept up in this torrent of activity as they seek to make clusters whose structures and properties approach those of bulk solids.[5] Indeed, the study of large clusters and small crystallites represents a bridge between molecular and solid-state chemistry. While molecular chemists synthesize transition-metal clusters resembling bulk metals and seek to understand them in molecular terms,[5,6] their solid-state counterparts try to understand the properties of small crystallites using concepts familiar from studies of extended solids.[7] Still other chemists find molecular clusters in solid-state compounds.[8] All of these workers—the molecular and the solid-state chemist, as well as the surface scientist who appeals to the surface-cluster analogy and organometallic chemistry to explain surface reactivity[9]—share a common desire to bridge solid-state and molecular chemistry.

The systems under study differ from the bulk solid as they lack translational symmetry: molecules adsorb on crystals interrupted by a surface; clusters and crystallites represent solids bounded by several surfaces. Our interest, spurred by a question from Boon Teo regarding the possibility of deriving molecular orbitals for large clusters,[10] rests in a theoretical description of chemical bonding in systems perturbed from perfect translational symmetry. Some examples are the raft-like clusters such as $Os_6(CO)_{17}\{P(OMe)_3\}_4$ or $Cu_5Fe_4(CO)_{16}^{3-}$, built from pieces of a two-dimensional, close-packed hexagonal net;[11] rhodium and platinum carbonyl clusters resembling pieces of hcp or fcc metals;[12] chains of face-sharing octahedra found in the Chevrel phases;[8g] or the metal–metal bonded oligomers based on the $Rh_2(L_2)_4^{n+}$ dimer.[13]

The clusters, or pieces-of-a-solid, mentioned above are fascinating in that they present us with a state of matter intermediate between the discrete molecule and the (almost) infinite solid. They are a *bridge*. At the same time as they are clearly important and

† Current address: Department of Chemistry, University of Houston, Houston, TX 77204-5641.

§ Permanent address: Quantum Chemistry Laboratory, Department of Chemistry, University of Warsaw, Pasteura 1, 02-093 Warsaw, Poland.

(1) Based on: Wheeler, R. A. Ph.D. Thesis, Cornell University, October 1987; Chapter II.

(2) (a) Steglich, F.; Aarts, J.; Bredl, C. D.; Lieke, W.; Meschede, D.; Franz, W.; Schaefer, H. *Phys. Rev. Lett.* **1979**, *43*, 1892. (b) Stewart, G. R. *Rev. Mod. Phys.* **1984**, *56*, 755. (c) Varma, C. M. *Comments Solid State Phys.* **1985**, *11*, 221.

(3) (a) Korshak, Yu. V.; Medvedeva, T. V.; Ovchinnikov, A. A.; Spector, V. N. *Nature (London)* **1987**, *326*, 370. (b) Torrance, J. B.; Oostra, S.; Nazzal, A. *Synth. Met.* **1987**, *19*, 709.

(4) (a) Bednorz, J. G.; Müller, K. *Z. Phys.* **1986**, *B64*, 18. (b) Chu, C. W.; Hor, P. H.; Meng, R. L.; Gao, L.; Huang, Z. J.; Wang, Y. Q. *Phys. Rev. Lett.* **1987**, *58*, 405.

(5) (a) Schmid, G. *Struc. Bonding (Berlin)* **1985**, *62*, 51. (b) Raithby, P. R. In *Transition Metal Clusters*; Johnson, B. F. G., Ed.; Wiley-Interscience: Chichester, 1980; p 5. (c) *Faraday Symp. Chem. Soc.* **1980**, *14*. (d) Proceedings of Third International Meeting on Small Particles and Inorganic Clusters. *Surf. Sci.* **1985**, *156*; Benneman, K. H., Koutecky, J., Eds.

(6) (a) Chini, P. *J. Organomet. Chem.* **1980**, *200*, 37. (b) Mingos, D. M. P.; Johnston, R. L. *Struc. Bonding (Berlin)*, in press. (c) Mingos, D. M. P. *J. Chem. Soc., Chem. Commun.* **1985**, 1352. (d) Mingos, D. M. P. *J. Chem. Soc., Chem. Commun.* **1983**, 706. (e) Koutecky, J.; Fantucci, P. *Chem. Rev.* **1986**, *86*, 539.

(7) See, for example: (a) Halperin, W. P. *Rev. Mod. Phys.* **1986**, *58*, 533. (b) Perenboom, J. A. A. J.; Wyder, P.; Meier, F. *Phys. Rep.* **1981**, *78*, 173. (c) Benfield, R. E.; Edwards, P. P.; Nelson, W. J. H.; Vargas, M. D.; Johnson, D. C.; Sienko, M. J. *Nature (London)* **1985**, *314*, 231. (d) Edwards, P. P.; Sienko, M. J. *Int. Rev. Phys. Chem.* **1983**, *3*, 83. (e) Baetzold, R. C.; Hamilton, J. F. *Prog. Solid State Chem.* **1983**, *15*, 1. (f) Cohen, M. L.; Chou, M. Y.; Knight, W. D.; de Heer, W. A. *J. Phys. Chem.* **1987**, *91*, 3141. (g) Davis, S. C.; Klabunde, K. J. *Chem. Rev.* **1982**, *82*, 53. (h) Mingos, D. M. P. *Chem. Soc. Rev.* **1986**, *15*, 31. (i) Teo, B. K. *J. Chem. Soc., Chem. Commun.* **1983**, 1362.

(8) (a) Simon, A. *Angew. Chem.* **1981**, *93*, 1. *Angew. Chem., Int. Ed. Engl.* **1981**, *20*, 1. (b) von Schnering, H.-G. *Angew. Chem.* **1981**, *93*, 44. *Angew. Chem., Int. Ed. Engl.* **1981**, *20*, 33. (c) Corbett, J. D., Ed. Proceedings of the Symposium on Metal–Metal Bonding in Solid State Clusters and Extended Arrays. In *J. Solid State Chem.* **1985**, *57*, 1. (d) Corbett, J. D., McCarley, R. E. In *Crystal Chemistry and Properties of Materials with Quasi-One-Dimensional Structures*; Rouxel, J., Ed.; D. Reidel: Dordrecht, 1986; p 179. (e) McCarley, R. E. *Philos. Trans. R. Soc. (London)* **1982**, *A308*, 141. (f) Corbett, J. D. *Acc. Chem. Res.* **1981**, *14*, 239. (g) Chevrel, R.; Sergent, M. In *Crystal Chemistry and Properties of Materials with Quasi-One-Dimensional Structures*; Rouxel, J., Ed.; D. Reidel: Dordrecht, 1986; p 315. (h) Schäfer, H.; von Schnering, H.-G. *Angew. Chem.* **1964**, *76*, 832.

0002-7863/88/1510-7302$01.50/0

structurally intriguing, they pose a problem to the theoretician. With modern orbital theories at his command, he can more or less easily calculate a discrete molecule (the monomer). And he can use the great simplifying aspect of perfect translational symmetry to do the extended three-dimensional material or polymer. But the medium-to-large cluster is tough. The $(Rh_2)_n$ oligomers,[13] Os rafts,[11] or Pt clusters[12] have enough orbitals to probe the limits even of the most economic (our extended Hückel) computer programs. At the same time it seems such a waste of effort to diagonalize a matrix the size of the number of orbitals of the full cluster when the chemical identity of the smaller problem (monomer or unit cell) is staring you right in the eye.

To extricate ourselves from "the oligomer bind", a perturbation method was developed to calculate the molecular orbitals of a cluster by starting with wave functions of the extended solid as the unperturbed, zeroth order solutions. The presentation emphasizes large, finite systems such as clusters and thin films, but the approach remains valid for the semi-infinite or infinite problems of surfaces, interfaces, and defects. The method relies heavily on the reciprocal space of finite crystals and its connection with the reciprocal lattice of the related infinite solid. This relationship is both a computational and a conceptual aid, for it provides a natural framework for discussing what are essentially big molecules using concepts and terminology from solid-state physics. It allows a direct comparison of molecules with solids and highlights their inherent similarities as well as differences brought about by the presence or absence of translational symmetry.

We begin this paper with a general theoretical discussion of localized and delocalized levels. The perturbation framework is set up and illustrated first with the example of a polyene and then with the $(Rh_2)_n$ oligomers. In a separate paper we provide a further application to finite chains of edge-sharing metal octahedra.[14]

Localized and Delocalized Levels

The infinite, periodic crystal is a fiction, invented by theoreticians to make calculations easier. Real crystals have boundaries and defects; the "infinite" polymer begins and ends. The theoretician's first approximation ignores these imperfections, wraps a periodic solid around on itself, and makes a tractable mathematical problem. Cyclic boundary conditions[15,16] thus reduce the infinite dimensional problem to a series of small calculations. The result is orbitals delocalized over the entire, extended system.

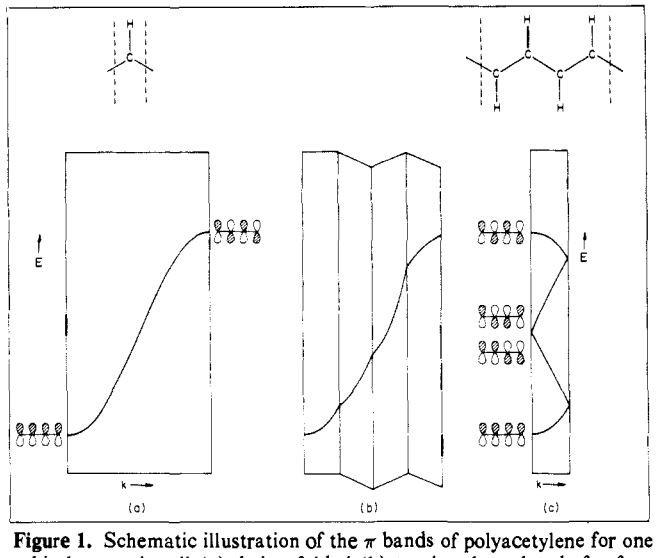

Figure 1. Schematic illustration of the π bands of polyacetylene for one orbital per unit cell (a), being folded (b) to give the π bands for four orbitals per cell (c).

Two difficulties arise when boundaries, defects, or other deviations from perfect periodicity become the focus of attention. First, localized levels are introduced in addition to the delocalized orbitals inherent in the periodic system. These additional levels are localized near the defect or surface and modify the properties of such compounds. The problem arises because localized levels are important, but they are difficult to calculate for the perturbed periodic system. The delocalized levels also present a problem in these systems, for translational symmetry with all its simplifying features is lost, and some other way is needed to reduce the size of the calculation. One common simplifying assumption represents defects or surfaces as local perturbations and involves a Green's function approach to calculate localized states.[17] Some delocalized levels could, in principle, be calculated as well, but this is typically not done.

An alternative approach described here is based on the perturbation of delocalized crystal orbitals to derive both the extended states and the localized levels due to defects, interfaces, or surfaces.[18] Clearly, the approach is valid only for systems showing approximate translational symmetry. Specific areas of application are broad, however, and include high nuclearity transition metal clusters, surface states, thin films, chemisorption on surfaces and on thin films, semiconductor superlattices, and defects in polymers and semiconductors. It is easiest to discuss the procedure, which is general and applicable to any orbital method, in the context of a specific problem, treated by the extended-Hückel method.[19]

(9) (a) Muetterties, E. L. *Chem. Soc. Rev.* **1982**, *11*, 283. (b) Muetterties, E. L.; Rhodin, T. N.; Rand, E.; Brucker, C. F.; Pretzer, W. R. *Chem. Rev.* **1979**, *79*, 91. (c) Canning, N. D. S.; Madix, R. J. *J. Phys. Chem.* **1984**, *88*, 2437. (d) Koestner, R. J.; Van Hove, M. A.; Somorjai, G. A. *J. Phys. Chem.* **1983**, *87*, 203.

(10) Teo, B. K., private communication.

(11) (a) Goudsmit, R. J.; Johnson, B. F. G.; Lewis, J.; Raithby, P. R.; Whitmire, K. A. *J. Chem. Soc., Chem. Commun.* **1982**, 640. (b) Doyle, G.; Eriksen, K. A.; Van Engen, D. *J. Am. Chem. Soc.* **1986**, *108*, 445. (c) Longoni, G.; Manassero, M.; Sansoni, M. *J. Am. Chem. Soc.* **1980**, *102*, 7973. (d) Freeman, M. J.; Miles, A. D.; Murray, M.; Orpen, A. G.; Stone, F. G. A. *Inorg. Chim. Acta* **1984**, *3*, 1093. (e) Bachechi, F.; Ott, J.; Venanzi, L. M. *J. Am. Chem. Soc.* **1985**, *107*, 1760. (f) Fajardo, M.; Holden, H. D.; Johnson, B. F. G.; Lewis, J.; Raithby, P. R. *J. Chem. Soc., Chem. Commun.* **1984**, 24.

(12) Some examples include the molecules described in: (a) Albano, V. G.; Ceriotti, A.; Chini, P.; Ciani, G.; Martinengo, S.; Anker, W. M. *J. Chem. Soc., Chem. Commun.* **1975**, 859. (b) Albano, V. G.; Ciani, G.; Martinengo, S.; Sironi, A. *J. Chem. Soc., Dalton Trans.* **1979**, 978. (c) Ciani, G.; Sironi, A.; Martinengo, S. *J. Chem. Soc., Chem. Commun.* **1981**, 519. (d) Ciani, G.; Magni, A.; Sironi, A.; Martinengo, S. *J. Chem. Soc., Chem. Commun.* **1981**, 1280. (e) Martinengo, S.; Ciani, G.; Sironi, A.; Chini, P. *J. Am. Chem. Soc.* **1978**, *100*, 7096. (f) Martinengo, S.; Ciani, G.; Sironi, A. *J. Am. Chem. Soc.* **1980**, *102*, 7564. (g) Vidal, J. L.; Schoening, R. C.; Troup, J. M. *Inorg. Chem.* **1981**, *20*, 227. (h) van der Linden, J. G. M.; Paulissen, M. L. H.; Schmitz, J. E. J. *J. Am. Chem. Soc.* **1983**, *105*, 1903. (i) Ciani, G.; Sironi, A.; Martinengo, S. *J. Organomet. Chem.* **1980**, *192*, C42. (j) Martinengo, S.; Ciani, G.; Sironi, A.; Chini, P. *J. Chem. Soc., Chem. Commun.* **1980**, 1140.

(13) (a) Cotton, F. A.; Walton, R. A. *Multiple Bonds Between Metal Atoms*; Wiley-Interscience: New York, 1982; Chapter 7. (b) Felthouse, T. R. *Prog. Inorg. Chem.* **1982**, *29*, 73.

(14) (a) Wheeler, R. A. Ph.D. Thesis, Cornell University, October 1987; Chapter III. (b) Wheeler, R. A.; Hoffmann, R. *J. Am. Chem. Soc.*, following paper in this issue.

(15) (a) Born, M.; von Karman, T. *Phys. Z.* **1913**, *14*, 15. (b) Born, M.; von Karman, T. *Phys. Z.* **1913**, *14*, 65.

(16) See also, e.g.: (a) Ashcroft, N. W.; Mermin, N. D. *Solid State Physics*; Holt, Rinehart, and Winston: Philadelphia, 1976. (b) Altmann, S. *Band Theory of Metals*; Pergamon: Oxford, 1970. (c) Callaway, J. *Energy Band Theory*; Academic: New York, 1964.

(17) See, for example: (a) Koster, G. F.; Slater, J. C. *Phys. Rev.* **1954**, *95*, 1167. (b) Callaway, J. *J. Math. Phys.* **1964**, *5*, 783. (c) Kalkstein, D.; Soven, P. *Surf. Sci.* **1971**, *26*, 85. (d) Davison, S. G.; Levine, J. D. In *Solid State Physics*; Ehrenreich, H., Seitz, F., Turnbull, D., Eds.; Academic: New York, 1970; Vol. 25, p 1. (e) Koutecky, J. *Adv. Chem. Phys.* **1965**, *9*, 85. (f) Stoneham, A. M. *Theory of Defects in Solids*; Clarendon: Oxford, 1975; Chapter 5. (g) Bullett, D. W.; Haydock, R.; Heine, V.; Kelley, M. J. In *Solid State Physics*; Ehrenreich, H., Seitz, F., Turnbull, D., Eds.; Academic: New York, 1980; Vol. 35. (h) Garcia-Moliner, F.; Velasco, V. R. *Prog. Surf. Sci.* **1986**, *21*, 93.

(18) Others have, in a similar spirit, derived analytical expressions for the Hückel MOs of large, finite clusters formed from simple cubic, bcc, or fcc metals: (a) Baldock, G. R. *Proc. Phys. Soc. (London)* **1953**, *A66*, 2. (b) Messmer, R. P. *Phys. Rev.* **1977**, *B15*, 1811. (c) Bilek, O.; Kadura, P. *Phys. Status Solidi* **1978**, *B85*, 225. (d) Bilek, O.; Skala, L. *Czech. J. Phys.* **1978**, *B28*, 1003. (e) Salem, L.; LeForestier, C. *Surf. Sci.* **1979**, *82*, 390. (f) Salem, L.; LeForestier, C. *J. Am. Chem. Soc.* **1985**, *107*, 2526. (g) Salem, L. *J. Phys. Chem.* **1985**, *89*, 5576.

(19) (a) Hoffmann, R.; Lipscomb, W. N. *J. Chem. Phys.* **1962**, *36*, 2179. (b) Hoffmann, R. *J. Chem. Phys.* **1963**, *39*, 1397.

Suppose we want the orbitals of butadiene, C_4H_6 (**1a**), and we have available to us the orbitals of polyacetylene—$(CH)_\infty$, **1b**. (Now this is patently silly, as an example, for the orbitals of butadiene are easily calculable.[20] It is not so silly when we want the orbital of $[Ni_3(CO)_3]_{18}^{2-}$...). The method begins with a band calculation for a small unit cell of the infinite chain model for *trans*-polyacetylene shown in **1b**. Next, the unit cell is enlarged. This is represented in **1c** and is a preparation for cutting out the

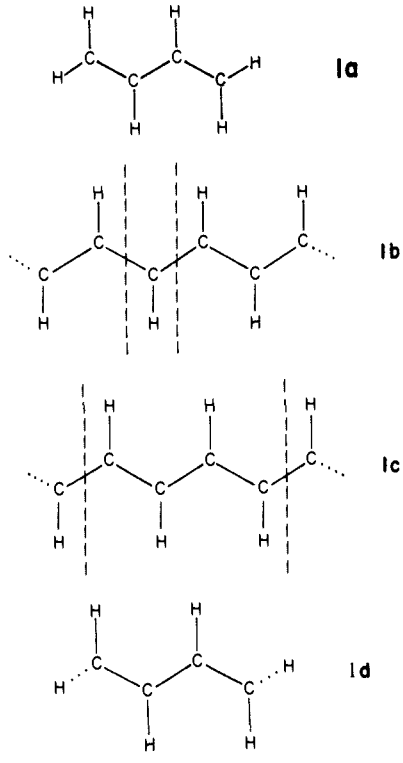

oligomer from the polymer. The orbitals for the large unit cell are conveniently derived from those of the small unit cell using simple band theory. The energy bands of the large unit cell are related to those of the small unit cell by a band folding mnemonic schematically illustrated in Figure 1 and described in many places in the literature.[21] Figure 1a shows the schematic π band of polyacetylene with one CH unit in the unit cell; Figure 1b shows the first Brillouin zone being cut to one-fourth its former size as the unit cell is quadrupled. In Figure 1c, when the unit cell has been quadrupled, there are four π bands at each k point within the Brillouin zone. The orbitals are drawn out at the zone center, $k = 0$, and correspond roughly to the π MO's of butadiene. The lowest energy orbital is totally bonding, the next two are singly and doubly noded within the unit cell, and the highest energy orbital is the most antibonding combination of the four π orbitals.

The next problem is in fact to cut out the oligomer from the polymer, making four orbitals out of the myriad available in the polymer. The four orbitals shown in Figure 1c are not the best or most representative ones for approximating the oligomer eigenfunctions. The problem, when we analyze it, will separate naturally into two parts: (1) Approximate delocalized states are taken from selected k points in a band calculation. k points are chosen so that (within the unit cell) the crystal orbitals mimic the nodal structure of the oligomer MO's but do not necessarily fall off correctly near the ends of the molecule. The choice of k points corresponds to choosing the part of the basis set on atoms common to the cluster and the large unit cell of the solid. (2) Crystal orbitals are mixed with each other and with orbitals of end-capping ligands, to give oligomer MO's as linear combinations of crystal orbitals (LCCO's). The procedure requires no more effort than that needed to perform separate MO and band calculations, but it provides a natural framework for interpreting cluster wave functions.

Some interesting problems will arise in selecting the appropriate k points, and these will be resolved by exploiting the relationship between the reciprocal space of finite and infinite crystals. The final step in the MO calculation is illustrated in **1d** and involves adding to the calculation the orbitals located on atoms which cap the ends of the oligomer. This will be accomplished by a perturbation theoretic formalism. Let us begin with the general setup of the problem.

Oligomer MO's from Polymer Crystal Orbitals

Our first problem is to derive oligomer MO's from symmetry orbitals of a related, infinite solid. We begin by finding symmetry-adapted linear combinations (SALC's) of atomic orbitals for a solid from a projection operator, in the same way that SALC's for a cyclic molecule can be derived.[22] The projection operator for the kth irreducible representation is given by a symmetry operator, $\hat{R}$, multiplied by the character of $\hat{R}$ in the kth irreducible representation, summed over all operations. The normalized projection operator is

$$\hat{P}_k = l_k/h \sum_R \Gamma_k(\hat{R})\hat{R} \qquad (1)$$

(l_k is the dimension of the irreducible representation and h is the dimension of the group). When applied to an arbitrary function χ_m, $\hat{P}_k$ projects out that part of the function transforming according to the kth irreducible representation. For a cyclic molecule, symmetry operations are rotations about the high-symmetry axis; for an infinite solid the symmetry operations consist of translations by a distance a. If the solid is large enough to neglect end effects,[23] an assumption formally expressed by using cyclic boundary conditions, all characters become complex exponentials. If one orbital of the infinite solid, a carbon p_z for example, is centered at each site, the projection operator can be applied to one function to give

$$\phi_k = \hat{P}_k\chi_0 = \sum_n e^{ikna}\chi_n \qquad (2)$$

The form of eq 2, the symmetry orbitals of the infinite solid, is the same as that for cyclic molecules if $k = 2\pi r/Na$, where r is a quantum number labeling the rth MO.

Equation 2 represents a general form for symmetry orbitals of an infinite solid, called Bloch functions.[16,21] Bloch functions for the solid serve the same convenient purpose as symmetry orbitals of a molecule: they give a Hamiltonian matrix factored into non-interacting blocks indexed by the symmetry label k. Each block has a dimension equal to the number of orbitals in the unit cell of the solid and there are as many k values (blocks) as there are unit cells in the macroscopic crystal. The problem of diagonalizing a matrix of infinite (or at least very large) dimension is thus reduced to solving a number of smaller problems, one for each value of k. For the π orbitals of polyacetylene, the Bloch functions are the same as the crystal orbitals and the Hamiltonian matrix is already diagonal. Although band structures can become quite complicated for large unit cells, within the tight-binding

(20) (a) Salem, L. *Molecular Orbital Theory of Conjugated Systems*; W. A. Benjamin: New York, 1966. (b) Heilbronner, E.; Bock, H. *The HMO Model and its Applications—1: Basis and Manipulation*; Wiley-Interscience: London, 1968.

(21) (a) Gerstein, B. C. *J. Chem. Educ.* **1973**, *50*, 316. (b) Burdett, J. K. *Prog. Solid State Chem.* **1984**, *15*, 173. (c) Whangbo, M.-H. In *Crystal Chemistry and Properties of Materials with Quasi-One-Dimensional Structures*; Rouxel, J., Ed.; D. Reidel: Dordrecht, 1986; p 27. (d) Albright, T. A.; Burdett, J. K.; Whangbo, M.-H. *Orbital Interactions in Chemistry*; Wiley-Interscience: New York, 1985. (e) Hoffmann, R. *Angew. Chem.* **1987**, *99*, 871.

(22) (a) Cotton, F. A. *Chemical Applications of Group Theory*; Wiley-Interscience: New York, 1971. (b) Tinkham, M. *Group Theory and Quantum Mechanics*; McGraw-Hill: New York, 1964. (c) Lax, M. *Symmetry Principles in Solid State and Molecular Physics*; Wiley-Interscience: New York, 1974.

(23) Neglecting crystal end effects and using cyclic boundary conditions introduces a negligible error in the *distribution* of vibrational or electronic energy levels provided that the ratio of boundary points to lattice points is small. The effect on individual levels, however, was not investigated by: (a) Ledermann, W. *Proc. R. Soc. (London)* **1944**, *A182*, 362. (b) Peierls, R. E. *Proc. Natl. Sci. Acad. (India)* **1954**, *20*, 121.

(simple Hückel) approximation, energy vs k for one orbital per unit cell traces out a simple cosine curve (see Figure 1a).[16,21a-c]

The crystal orbitals with the energies shown in Figure 1a agree with chemical intuition. The completely bonding combination of carbon p_z orbitals ($k = 0$) has the lowest energy and the antibonding level ($k = \pi/a$) appears at high energy. The orbitals associated with k values between $k = 0$ and π/a have a nodal structure intermediate between the completely bonding and antibonding extremes. The π orbital of polyacetylene at $k = 0$ is shown in Figure 1a, where $\phi_{k=0} = \chi_1 + \chi_2 + \chi_3 + \ldots$ is the completely in-phase combination of carbon p_z. Figure 1a also shows $\phi_{k=\pi/a} = \chi_1 - \chi_2 + \chi_3 - \ldots$, the most antibonding crystal orbital.

The projection operator formalism and the sample wave functions shown in Figure 1a emphasize several of the more important characteristics of k values in band calculations: their function as symmetry labels and as node counters for crystal orbitals. A third crucial function of *k vectors*, their role in defining the reciprocal space of an extended solid, will be important later. For now, the more practical aspects of performing a band calculation require some explanation.

Since there are as many k values in Figure 1a as there are unit cells in the macroscopic crystal, it remains impossible to solve the eigenvalue problem at every value of k. By performing a band calculation at selected k points, however, it is possible to characterize the electronic structure of an extended solid. Several types of k points are typically preferred, depending on the type of information desired. k values located along high symmetry lines in the reciprocal space of the solid are chosen to plot energy bands,[16] whereas "special k point sets" are known to give optimum average values, such as the total energy of a solid-state compound.[24] Yet another set of k values seems to be required to answer a question that, to our knowledge, has never been asked before:[25] at which k point(s) do the crystal orbitals of a solid best represent the MO's of a related cluster?

Instead of comparing π orbitals of linear polyenes directly with polymer crystal orbitals, however, it proves convenient to consider as an intermediate step the MO's of the cyclic molecule. This is because symmetry labels for the cyclic molecule MO's correspond directly to k values for the infinite polymer with cyclic boundary conditions. The π orbitals of the cyclic molecule can be related, within a simple Hückel model, to the MO's of the finite chain. Thus the π orbitals of a finite polyene chain are contained in the π orbitals of the corresponding cyclic molecule, and the symmetries of the cyclic molecule orbitals tell which k values to choose for the corresponding band calculation. The cyclic molecule thus provides a key to choosing the correct k values to describe MO's of the finite chain molecule.

Let us look then at the energy levels and wave functions of a typical cyclic polyene, 10-annulene. The levels of 10-annulene will turn out to be related to those of butadiene. The π-levels of 10-annulene are given by eq 2, with $k = 2\pi r/Na$ for the rth MO and $N = 10$. The sum over sites, n, ranges from 0 to $N - 1$. Orbital energies for planar 10-annulene are shown in **2**, superimposed on the schematic π energy band of polyacetylene plotted from $k = -\pi/a$ to $+\pi/a$. (We should point out that our smallest unit cell for computations involving *trans*-polyacetylene contains *two* CH units, not one. This results in a different but analogous choice of k points for our numerical calculations presented later.)

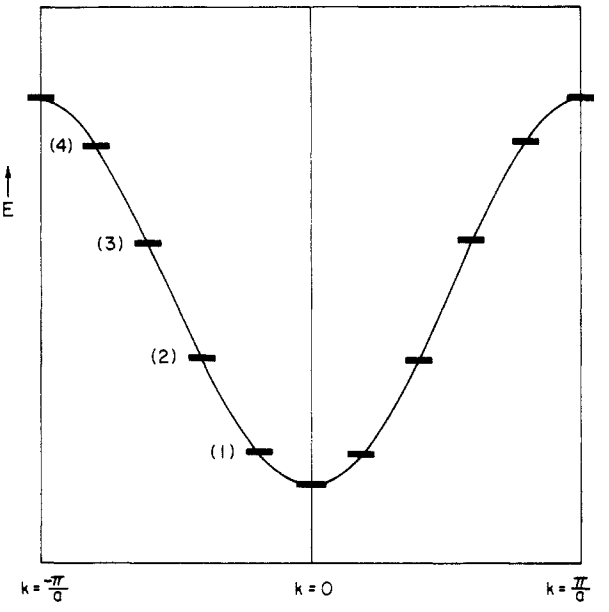

2

2 shows that the levels of cyclic molecules are contained in the band structure for the infinite polymer. The levels labeled 1–4 are a singly, doubly, and triply noded orbital of 10-annulene drawn out in **3**. These orbitals are antisymmetric with respect to a vertical mirror plane drawn as dashed lines in **3**. The curved, dotted lines in **3** emphasize that the π orbitals of the butadiene molecule are found in the levels of 10-annulene. At the simple Hückel level, the relationship is exact: orbital coefficients and energies for a chain of N p_z orbitals are contained in those for a cyclic molecule of $2N + 2$ atoms.[26] Thus, the energy bands of the infinite polymer of polyacetylene contain the π levels of cyclic hydrocarbons which, in turn, contain the π orbitals of smaller, linear chain polyenes. This simple relationship between the polymer π levels and the π orbitals of the cyclic molecule is exact, whereas that between the cyclic molecule and the linear molecule depends on two very restrictive assumptions: (1) zero overlap and (2) nearest-neighbor interaction only.

Whereas the previous discussion assumed one orbital per unit cell and thus only one band, any real solid will give rise to several bands, one for each atomic orbital in the unit cell. Furthermore, each crystal orbital will be composed of a combination of AO's with coefficients that vary with k in some complicated way. The complications will multiply still more when the cluster is cut from the solid, for the σ bands will be more violently perturbed than the π orbitals. The band calculation, though complicated, is not a real problem. By choosing appropriate k points from a band calculation it is possible to extend the (approximate) results of this section to other, more complex solid-state compounds and to calculate the orbitals for finite chain or cluster molecules. The close association between the reciprocal space of finite crystals and the reciprocal lattice of the infinite solid provides a key to k point selection for more complicated solids.

The Reciprocal Space of Finite Crystals

The tremendously useful construct of the reciprocal lattice of an infinite crystal[27] is a cornerstone of both modern crystallography

(24) (a) Chadi, D. J.; Cohen, M. L. *Phys. Rev.* **1973**, *B8*, 5747. (b) Monkhorst, H. J.; Pack, J. D. *Phys. Rev.* **1976**, *B13*, 5188. (c) Chadi, D. J. *Phys. Rev.* **1977**, *B16*, 1746. (d) Pack, J. D.; Monkhorst, H. J. *Phys. Rev.* **1977**, *B16*, 1748. (e) Evarestov, R. A.; Smirnov, V. P. *Phys. Status Solidi* **1983**, *B119*, 9. (f) Evarestov, R. A.; Petrashen, M. I.; Ledovskaya, E. M. *Phys. Status Solidi* **1975**, *B68*, 453. (g) Bandura, A. V.; Evarestov, R. A. *Phys. Status Solidi* **1974**, *B64*, 635. (h) Ramirez, R.; Böhm, M. C. *Int. J. Quantum Chem.* **1986**, *30*, 391. (i) Baldereschi, A. *Phys. Rev.* **1973**, *B7*, 5212. (j) Bashenov, V. K.; Bardashova, M.; Mutal, A. M. *Phys. Status Solidi* **1977**, *B80*, K89.

(25) Instead of using energy bands of a solid as the starting point for a cluster calculation, the converse has been tried—namely, the electronic structure of solids or surfaces is often approximated by using a cluster model. Some leading references include: (a) Upton, T. H.; Goddard, W. A., III *CRC Crit. Rev. Solid State Mater. Sci.* **1981**, *10*, 261. (b) Messmer, R. P. *Surf. Sci.* **1981**, *106*, 225. (c) Gavezzotti, A.; Simonetta, M. *Adv. Quantum Chem.* **1980**, *12*, 103. (d) Messmer, R. P. In *The Nature of the Surface Chemical Bond*; Rhodin, T. N., Ertl, G., Eds.; North-Holland: Amsterdam, 1979. (e) Messmer, R. P. In *Semiempirical Methods in Electronic Structure Calculations, Part B: Applications*; Segal, G. A., Ed.; Plenum: New York, 1977. (f) Burdett, J. K. In *Structure and Bonding in Crystals*; O'Keefe, M., Navrotsky, A., Eds.; Academic: New York, 1981; Vol. 1, pp 264ff. (g) Changhsing, Cui; Yuansheng, Jiang *Acta Phys.-Chim. Sinica* **1987**, *3*, 581. (h) Changhsing, Cui; Xiaotian, Li; Yuansheng, Jiang *Acta Chim. Sinica* **1987**, *45*, 840.

(26) See ref 20b, pp 131–139.

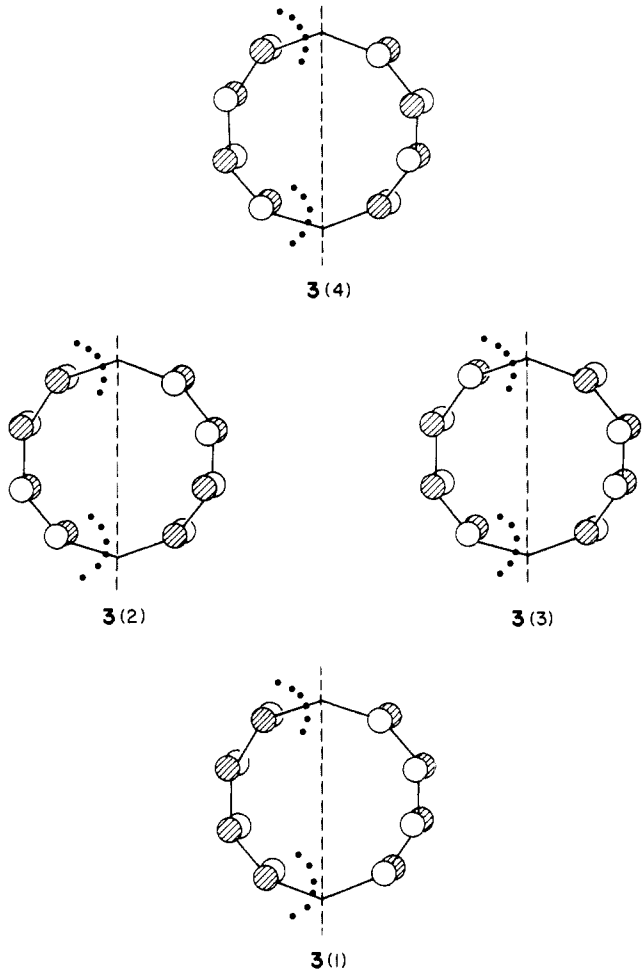

and solid-state physics. The direct geometrical relationship between the reciprocal lattice and the direct lattice[28] allows the crystallographer to build a crystal structure from its reciprocal space image, obtained in a diffraction experiment. In a similar way, the reciprocal space ("k space") of a solid provides a framework for understanding vibrational spectra and electronic structure of solids. A simple example was sketched in the preceding section. In addition, an average property of a solid such as the total electronic energy can be easily computed as a lattice sum in reciprocal space—a sum of its values at selected k points. All of these conveniences, both computational and conceptual, result directly from the reciprocal space concept for the infinite crystal.

For large but finite crystals, the reciprocal space is preserved, albeit in modified form. The nature of these modifications[29] and their implications for some concepts of solid-state chemistry are the subject of this section and the next. The form of the reciprocal space will be introduced first; then lattice sums such as Bloch functions or total electronic energy will be considered for the truncated crystal. The resulting lattice sums are simply related to those of the infinite solid. This relationship suggests a recipe for selecting k points from the band calculation for the infinite crystal where crystal orbitals best represent cluster MO's. Before discussing the selection of k points for the cluster calculation, however, it is appropriate to comment on the modified form of the reciprocal space of a finite crystal.

The reciprocal lattice of an infinite solid can be derived from the corresponding direct lattice by a simple Fourier transform. First, the direct lattice of an infinite array of discrete points is represented mathematically by the lattice function, $\mathbf{G}(\vec{r})$

$$\mathbf{G}(\vec{r}) = \sum_{R_\alpha} \delta(\vec{r} - \vec{R}_\alpha) \tag{3}$$

The δ function in eq 3 represents a lattice point, whereas the sum over direct lattice vectors, $\vec{R}_\alpha$, serves to propagate the point to other sites of the lattice. The reciprocal space image of the lattice function is the Laue function, $L_\infty(k) = |Z_\infty|^2$, where Z_∞ is the scattering amplitude of the point lattice. Since the scattering amplitude for the infinite lattice, Z_∞, is just the Fourier transform of $\mathbf{G}$,[29] the Laue function is simply given by

$$L_\infty(\vec{k}) = \sum_{R_\beta}\sum_{R_\alpha} \exp(i\vec{k}\cdot(\vec{R}_\alpha - \vec{R}_\beta)) \tag{4}$$

This double sum is zero unless $\vec{k}\cdot(\vec{R}_\beta - \vec{R}_\alpha)$ is an integer multiple of 2π, a requirement that restricts $\vec{k}$ to reciprocal lattice vectors, $\vec{K}_\alpha$. $L_\infty(\vec{k})$ thus reduces to

$$L_\infty(\vec{k}) = \sum_\alpha \delta(\vec{k} - \vec{K}_\alpha) \tag{5}$$

Equation 5 expresses the familiar result that the reciprocal lattice of a point lattice is also a lattice of points. **4** shows the reciprocal

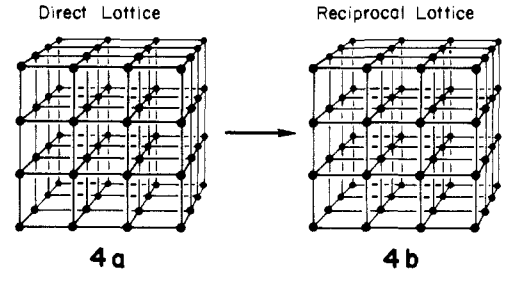

lattice for a simple cubic point lattice. Since reciprocal lattice vectors are orthogonal to direct lattice vectors, reciprocal lattice **4b** is also a simple cubic lattice of points.

The shape of a finite-size crystal can be accounted for by weighting each lattice point by a shape function $S(\vec{r})$

$$\mathbf{G}(\vec{r}) = \sum_\alpha S(\vec{r})\delta(\vec{r} - \vec{R}_\alpha) \tag{6}$$

For a large enough crystal, the reciprocal space image corresponding to eq 6 now depends on the crystal shape according to

$$L_N = \sum|\tilde{S}(\vec{k} - \vec{K}_\alpha)|^2 \tag{7}$$

Equation 7 gives the form of the reciprocal space for the finite crystal: an array of objects representing the crystal's macroscopic form, rather than a lattice of points.

To illustrate the form of the reciprocal space for a finite crystal, the Fourier transform of $\mathbf{G}(\vec{r})$ can be calculated explicitly for a given crystal geometry. This has been done to derive reciprocal space images for crystals with most common polyhedral shapes.[30] The result is particularly simple for a parallelopiped with relative edge lengths of N_1, N_2, and N_3:[30]

$$L_N = V^2N^2 \sin^2(\pi N_1k_x)/(\pi N_1k_x)^2 \sin^2(\pi N_2k_y)/(\pi N_2k_y)^2 \sin^2(\pi N_3k_z)/(\pi N_3k_z)^2 \tag{8}$$

where $VN = VN_1N_2N_3$ is the volume of the crystal. The function $\sin^2 x/x^2$ has the simple form illustrated in **5**. The principal maximum in **5** is much larger than the secondary maxima, so that the function's first zero defines its approximate width. The first zero occurs at $k_x = 1/N_1a$, where N_1a is the length of the crystal's edge. The result for a rectangular box of simple cubic crystal (**6a**)

(27) The reciprocal space was first introduced by: (a) Ewald, P. P. *Phys. Z.* **1913**, *14*, 465, 1038. (b) von Laue, M. *Jahrb. Radioakt. Elektron.* **1917**, *11*, 308. (c) See also: Ewald, P. P. *Z. Kristallogr.* **1936**, *93*, 396.

(28) Ewald, P. P. *Z. Kristallogr.* **1921**, *56*, 129.

(29) The reciprocal space of finite crystals is a familiar concept in crystallography and is discussed in: (a) James, R. W. *The Optical Principles of the Diffraction of X-Rays*; Cornell University: Ithaca, 1965. (b) Guinier, A. *Theorie et Technique de la Radiocristallographie*; Dunod: Paris, 1964. (c) Cowley, J. M. *Diffraction Physics*; North-Holland: Amsterdam, 1981.

(30) (a) von Laue, M. *Ann. Phys. (Paris)* **1936**, *26*, 55. (b) Ewald, P. P. *Proc. Phys. Soc. (London)* **1940**, *52*, 167. (c) Patterson, A. L. *Phys. Rev.* **1939**, *56*, 972. (d) Ino, T.; Minami, N. *Acta Crystallogr.* **1979**, *A35*, 163.

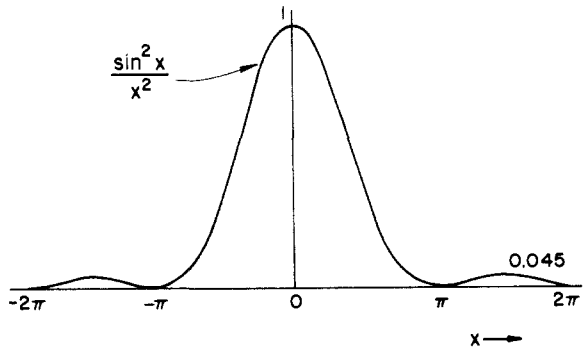

5

is a reciprocal space composed of parallelopipeds with sides $1/N_1a$, $1/N_2a$, and $1/N_3a$ in length and shown in **6b**. The effect of finite

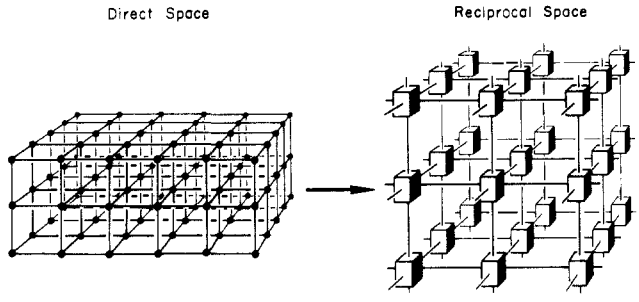

6a **6b**

crystal size shown in **5** and **6b** is experimentally observed as a broadening of diffraction peaks, but resolution is usually insufficient to see the structure in the peaks due to crystal shape. In the following, a general shape function, $s_\alpha = 1$ for the point $\alpha = l$ inside the finite crystal and $s_\alpha = 0$ for $\alpha = l$ outside, is used. Such a shape function serves to cut the cluster from the solid by truncating the sum of eq 6 at the crystal boundaries.

The shape function s_α provides a way to account for the effect of finite crystal size on lattice sums important in determining the properties of solids. Bloch functions provide one example of a lattice sum. They were discussed before for the one-dimensional case and are given in general by a sum over the direct lattice (indexed by lattice vectors $\vec{R}_\alpha$) of a complex exponential multiplied by an orbital centered at the site $\vec{R}_\alpha$

$$\Psi_\infty(\vec{k}) = \sum_{\vec{R}_\alpha=-\infty}^{\infty} \exp(i\vec{k}\cdot\vec{R}_\alpha)\chi(\vec{r} - \vec{R}_\alpha) \qquad (9)$$

Equation 9 could be expressed equally well as a series in sines or in cosines. Furthermore, orbitals represented by the cosine series differ from those expressed as sines by a 90° phase factor. Approximate molecular orbitals of the N atom crystal, Ψ_N, are derived by cutting the cluster from the solid. Truncating the crystal is achieved analytically by a trick of Fourier analysis, by convoluting $\Psi_\infty(\vec{k})$ with the shape function Z_N, where

$$Z_N = \sum_{\alpha=-\infty}^{\infty} S_\alpha \exp(i\vec{k}\cdot\vec{R}_\alpha) \qquad S_\alpha = 1,\ \alpha = l;\ 0,\ \alpha \neq l \qquad (10)$$

The result is

$$\Psi_N = \int \Psi_\infty(\vec{k}')Z_N(\vec{k} - \vec{k}')\, d\vec{k}' = \sum_{\alpha,\beta}\chi_\alpha \exp(i\vec{k}\cdot\vec{R}_\alpha)s_\beta\delta_{\alpha,\beta} = \sum_{n=-N/2}^{N/2}\chi_n \exp(i\vec{k}\cdot\vec{R}_n) \qquad (11)$$

where the origin is at the center of the finite crystal. Equation 11 involves a sum only over the N atoms in the cluster and is simply the formal expression for the part of the crystal orbital that is located on atoms within the cluster. The sum over $\vec{R}_n$, for a crystal with the shape of a parallelopiped, can be expressed as a product of sine series

$$\Psi_N = \sum_{n_1=-N_1/2}^{N_1/2} \sin(x_{n_1}k_x) \sum_{n_2=-N_2/2}^{N_2/2} \sin(y_{n_2}k_y) \sum_{n_3=-N_3/2}^{N_3/2} \sin(z_{n_3}k_z)\chi_{n_1n_2n_3} \qquad (12)$$

The form of eq 12 both reflects the finite nature of the crystal and agrees with published results for the Hückel orbitals of a finite, cubic cluster.[18] The k vector in eq 11 refers to a point in the reciprocal space of the infinite crystal and remains to be determined.

k Points for Clusters

At this point there are at least two ways, both leading to the same result, to find k values where orbitals of the extended solid will give a good approximation to Ψ_N, the MO's of the N atom cluster. One way is to consider the relation between Hamiltonians for the finite and infinite crystals, H_N and $H_\infty(\vec{k})$. The second method involves building an infinite crystal from unit cells containing the cluster and asking how to derive orbitals of the solid, assuming that cluster MO's are known. For the first method, H_N and $H_\infty(\vec{k})$ are simply related, as the wave functions Ψ_N and Ψ_∞ are related, by a convolution integral

$$H_N = \int H_\infty(\vec{k} - \vec{k}')L_N(\vec{k}')\, d\vec{k}' \qquad (13)$$

where the Laue factor is $L_N(k) = |Z_N|^2$. Equation 13 reduces to give an expression relating H_N to H_∞

$$H_N = H_\infty(\vec{k}) \int \exp(i\vec{k}'\cdot(\vec{R}_\alpha - \vec{R}_{\alpha'}))L_N(\vec{k}')\, d\vec{k}' \qquad (14)$$

with

$$H_\infty(\vec{k}) = \sum_{\alpha,\alpha'} \exp(i\vec{k}\cdot(\vec{R}_\alpha - \vec{R}_{\alpha'}))\langle\chi_{\alpha'}|H|\chi_\alpha\rangle$$

The total energy expressed as a sum over k becomes

$$E = \sum_k\{\sum_{\alpha,\alpha'} \exp(i\vec{k}\cdot(\vec{R}_\alpha - \vec{R}_{\alpha'})) \langle\chi_{\alpha'}|H|\chi_\alpha\rangle\}\int \exp(i\vec{k}'\cdot(\vec{R}_\alpha - \vec{R}_{\alpha'}))L_N(\vec{k}')\, d\vec{k}' \qquad (15)$$

Equation 15 consists of two parts. The first term, the term in curly brackets, is the expression for the energy of an infinite crystal. The second term contains all the information regarding crystal size and shape. This term represents a definite integral over points $\vec{k}'$ which are within the object enclosing a reciprocal lattice point of the infinite crystal (e.g., parallelopipeds, see **6**). The energy expression for a finite crystal consists of the same terms appearing in the energy expression for the infinite crystal, but weighted to account for the smearing out of lattice points. The form of eq 15 shows that optimum k points for the finite crystal are the same as optimum k points for the infinite solid. In other words, the problem of choosing k points for the finite cluster reduces to the same type of interpolation problem for the infinite solid as the one whose solution is well-known as "representative" or "special" k point sets.[24] In particular, the large unit cell method[24e-h] of special k point selection graphically illustrates the process of choosing k points for clusters. It involves enlarging a small unit cell to reduce the size of the Brillouin zone and to bring the desired k points to the Γ point, $k = 0$, for the new Brillouin zone. **7a** and **7b** show schematically how the process works for generating one particular set of four special k points. The unit cell for the one-band problem is enlarged by a factor of 10 (there are ten bands in **7b**) to map the four circled points in **7a** back to the point $k = 0$ (**7b**). The four k points chosen as special k points from **7a** therefore coincide exactly with the four k points of **2** which give the orbitals of butadiene. Equation 15 implies, in general, that the optimum k points for an isolated oligomer containing N atoms are also optimum k points for a periodically repeated oligomer or large unit cell.

A second way to arrive at a method of choosing k points for the band calculation starts by conceptually building the extended solid from large unit cells, with each cell composed of a cluster.

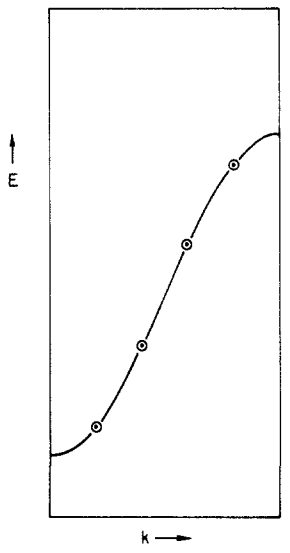

7a

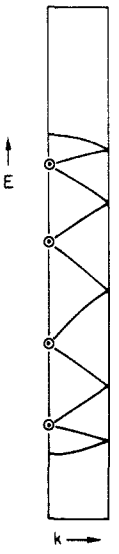

7b

Polyacetylene, for example, could be built from unit cells made up of a butadiene. The relevant question to ask now is which orbitals of the extended solid (polyacetylene) most closely resemble the orthogonal set of cluster (butadiene) MO's. If the orbitals of the solid are required to be orthogonal, the procedure for constructing orbitals of the solid that match the "MO's" of the unit cell most closely (in a least-squares sense) is well-known.[31] The procedure is called symmetric orthogonalization[32] and the resulting functions are Wannier functions for the solid. Since the Wannier functions are orthogonal functions localized[33] within the large unit cell corresponding to the cluster, this result makes intuitive sense. It says that orbitals of the solid which closely resemble cluster MO's are those orbitals that are localized on the part of the solid included in the cluster and having zero overlap with orbitals in neighboring unit cells. Of course, the Wannier functions may not be the best possible set of orbitals to reproduce cluster orbitals; they are simply the best *orthogonal* set. Relaxing the orthogonality constraint or using a criterion other than a least-squares fit to cluster MO's could give orbitals of the solid that represent a better guess for cluster MO's. Yet Wannier functions approximate cluster MO's more closely than other readily accessible orbitals of the infinite solid, such as Bloch functions or crystal orbitals.

The Wannier functions derived by this reasoning are related in a simple way to the crystal orbitals for a unit cell containing the cluster. Since one Wannier function is associated with each band and has an average energy defined at the middle of the band, the circled levels in **8a** correspond to crystal orbitals that most closely match the Wannier functions. **8b** shows the orbital derived from the lowest energy band and circled in **8a**. This orbital is completely bonding within the unit cell and noded with period 4a (a is a lattice vector for the small unit cell). Thus, the one k point approximation to Wannier functions is crystal orbitals that are isolated as much as possible from the rest of the crystal by their nonbonding nature with nearest neighbor cells. Using a larger k point set than the one in **8a** would mix crystal orbitals with

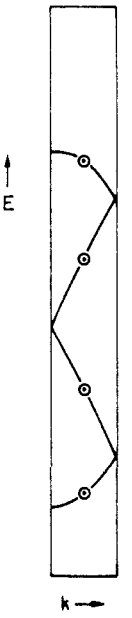

8a

different k values to diminish the crystal orbital amplitudes in more distant cells. The justification and the procedure for choosing other, larger k point sets to derive Wannier functions rests in the previously introduced notion of special k points.[24,34]

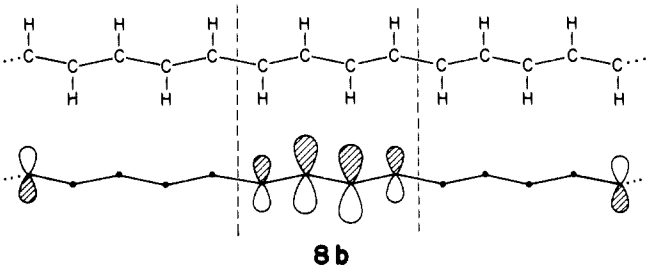

8b

Thus, the special k point sets familiar from the theory of infinite solids represent the best choice of k points for our problem, considered from two viewpoints: orbital energies or orbital amplitudes and nodal structure. Of the many possible special k point sets,[24] the ones that give the best Wannier functions should give the best cluster MO's. There has been some debate[24c-e] regarding the efficiency of the different k point sets and, although we have not done a systematic study, we have tested the several possibilities presented so far. For the polyenes and the Rh oligomers to be discussed later, one k point (in the Brillouin zone corresponding to the large unit cell) is sufficient to give good results. Although the points illustrated in **7b** and **8a** give similar results for the examples considered, selecting the mean value point[24i,j] for the large unit cell (e.g., **8a**) is a particularly straightforward choice for more complicated systems. Reference 24j lists mean value points for a variety of crystal symmetries.

We do not discuss here the implications of our analysis for the converse problem—how to model a surface by a finite cluster of atoms. We should emphasize, however, that the connection between the reciprocal spaces for the finite and infinite crystals means that the *shape*[35,36] as well as the size[37] of the cluster model is important.

(31) (a) Carlson, B. C.; Keller, J. M. *Phys. Rev.* **1957**, *105*, 102. (b) Pratt, G. W., Jr.; Neustadter, S. F. *Phys. Rev.* **1956**, *101*, 1248.

(32) (a) Landshoff, R. *Z. Phys.* **1936**, *102*, 201. (b) Löwdin, P.-O. *J. Chem. Phys.* **1950**, *18*, 365. (c) Löwdin, P.-O. *Adv. Phys.* **1956**, *5*, 49–54. (d) Löwdin, P.-O. *Adv. Quantum Chem.* **1970**, *5*, 185.

(33) (a) Wannier, G. H. *Phys. Rev.* **1937**, *52*, 191. (b) Kohn, W. *Phys. Rev.* **1959**, *115*, 809. (c) Des Cloizeaux, J. *Phys. Rev.* **1963**, *129*, 554. (d) Des Cloizeaux, J. *Phys. Rev.* **1964**, *135*, A685, A698. (e) Blount, E. I. In *Solid State Physics*; Seitz, F., Turnbull, D., Eds.; Academic: New York, 1962; Vol. 13, p 305.

(34) Chadi, D. J.; Cohen, M. L. *Solid State Commun.* **1973**, *13*, 1007.

(35) (a) LaFemina, J. P.; Lowe, J. P. *J. Am. Chem. Soc.* **1986**, *108*, 2527. (b) Minot, C.; Kahn, O.; Salem, L. *Surf. Sci.* **1980**, *94*, 15.

(36) (a) Evarestov, R. A.; Petrashen, M. I.; Ledovskaya, E. M. *Phys. Status Solidi* **1976**, *B76*, 377. (b) Dobrotvorskii, A. M.; Evarestov, R. A. *Phys. Status Solidi* **1974**, *66*, 83. (c) Zunger, A. *J. Phys.* **1974**, *C7*, 96. (d) Zunger, A. *Phys. Rev.* **1975**, *B11*, 2378. (e) Newman, D. J. *J. Phys. Chem. Solids* **1974**, *35*, 1187. (f) Watkins, G. D.; Messmer, R. P. In *Computational Methods for Large Molecules and Localized States in Solids*; Herman, F., McLean, A. D., Nesbet, R. K., Eds.; Plenum: New York, 1973; p 133.

(37) Cioslowski, J.; Kertesz, M. *J. Chem. Phys.* **1986**, *85*, 7193.

Cluster MO's from Crystal Orbitals of a Solid

The effect of solving for cluster MO's with a crystal orbital basis, chosen according to the procedure just described, can be seen by comparing the Hamiltonian matrices for the solid and for the cluster. In a basis of crystal orbitals, the Hamiltonian matrix of the solid is diagonal, but cutting the cluster from the solid introduces small, off-diagonal elements. The resulting matrix—with its diagonal elements large compared to its off-diagonal elements—remains diagonally dominant. Adding the orbitals of capping atoms slightly complicates the picture, but the final result is a Hamiltonian matrix for the cluster that is approximately diagonal and easily handled by numerical methods akin to perturbation theory.

Both perturbation theory and the related numerical methods used here to solve the molecular eigenvalue problem evolve from a matrix partitioning technique developed for problems in quantum chemistry by Löwdin.[38,39] In the partitioning technique, the matrix eigenvalue equation for the molecule

$$\mathbf{Mc} = (\mathbf{H} - E\mathbf{S})\mathbf{c} = 0 \tag{16}$$

is divided into two parts, a and b

$$\begin{pmatrix} \mathbf{M}_{aa} & \mathbf{M}_{ab} \\ \mathbf{M}_{ba} & \mathbf{M}_{bb} \end{pmatrix} \begin{pmatrix} \mathbf{C}_a \\ \mathbf{C}_b \end{pmatrix} = 0 \tag{17}$$

The partitioning gives two coupled matrix equations

$$\mathbf{M}_{aa}\mathbf{c}_a + \mathbf{M}_{ab}\mathbf{c}_b = 0 \tag{18}$$

and

$$\mathbf{M}_{ba}\mathbf{c}_a + \mathbf{M}_{bb}\mathbf{c}_b = 0 \tag{19}$$

Equation 19 can be solved for $\mathbf{c}_b$

$$\mathbf{c}_b = -\mathbf{M}_{bb}^{-1}\mathbf{M}_{ba}\mathbf{c}_a \tag{20}$$

and the result substituted into eq 18 to give

$$\bar{\mathbf{M}}_{aa}\mathbf{c}_a = (\mathbf{M}_{aa} - \mathbf{M}_{ab}\mathbf{M}_{bb}^{-1}\mathbf{M}_{ba})\mathbf{c}_a = 0 \tag{21}$$

Inverting the matrix $\mathbf{M}_{bb}$ presents the major computational barrier to solving eq 20 and 21 and has been considered in detail by several authors. The methods considered include a variety of familiar quantum mechanical approximation methods. Among the methods considered by Löwdin,[39d,40] for example, is a power series expansion of $(\mathbf{H}_{bb} - E\mathbf{S}_{bb})^{-1}$ that is equivalent to Brillouin–Wigner perturbation theory.[41] Alternatively, if $\mathbf{H}_{ba}$ is regarded as a perturbing potential V, $(\mathbf{H}_{bb} - E\mathbf{S}_{bb})^{-1}$ can be identified as a Green's function.[42] The usual Green's function approach uses localized wave functions and the short range of the perturbing potential to reduce the size of matrix eq 20 and 21 to a manageable size. The Hamiltonian matrix for the smaller problem is then diagonalized with any one of several standard diagonalization routines.[43]

In contrast to the usual Green's function methods, the present treatment uses delocalized orbitals (plus orbitals on end-capping atoms) as basis functions. Instead of using the short range of the perturbation to truncate the system of equations, the connection with perturbation theory is exploited: as in perturbation theory, the energy denominator $(\mathbf{H}_{bb} - E\mathbf{S}_{bb})^{-1}$ determines which orbital coefficients will be small. Since the starting eigenvectors are close approximations to the oligomer MO's, those orbitals far away in energy from the energy of the dominant crystal orbital could be neglected. Instead of simply truncating the system of equations, however, Brillouin–Wigner perturbation theory can be repeatedly applied to diagonalize the Hamiltonian matrix. The numerical method that incorporates Brillouin–Wigner perturbation theory is a common iterative technique for finding several roots of large, sparse matrices called the relaxation method. Although the matrices used here are not sparse, they are large and diagonally dominant. Consequently, iterative methods in general, and the relaxation method in particular, should work nearly as well for finding cluster MO's as for finding the eigenvalues of sparse matrices.

For sparse or diagonally dominant, large matrices, iterative methods are preferable to direct methods for finding several eigenvalues and eigenvectors because they do not use similarity transformations. Therefore, iterative methods have the advantages of maintaining matrix sparsity and of requiring approximately N^2 operations per eigenvalue instead of the N^3 operations required to diagonalize an $N \times N$ matrix.[44] The savings in cost and time have made iterative methods attractive in quantum chemistry for large configuration interaction (CI) calculations.[45] The usual procedure involves minimizing the Rayleigh quotient by coordinate relaxation[46] to find only the lowest eigenvalue. Shavitt et al. have subsequently extended the technique to find several higher eigenvalues by their method of optimal relaxation.[46d]

In its simplest form, coordinate relaxation proceeds by fixing one set of eigenvector components, c_a, and folding in the contributions from other components, c_b, one at a time. In the first iteration, the dimension of $\mathbf{M}_{aa}$ in eq 21 grows by one as each component is added. The matrix $\mathbf{M}_{bb}$, on the other hand, always has one component. On an element level, each iteration corresponds to incrementing the c_b's one at a time according to the scheme

$$\sigma_b = \sum_i H_{bi}c_i - E\sum_i S_{bi}c_i \tag{22}$$

$$\Delta c_b = \sigma_b/(ES_{bb} - H_{bb}) \tag{23}$$

$$c_b^{(k+1)} = c_b^{(k)} + \Delta c_b^{(k+1)} \tag{24}$$

where the index i refers to basis functions in set a. A new guess for the energy can be computed from the new c_b and the process continued. This corresponds to repeated application of Brillouin–Wigner perturbation theory.

Solving eq 16 for transition-metal clusters by coordinate relaxation resulted in severe convergence difficulties when two eigenvalues were within 0.2 eV of each other.[47] Modification such as overrelaxation or underrelaxation, involving multiplying the correction vector by a factor ω $(0 < \omega < 2)$,[48] changed the

(38) Early contributions to the partitioning method were made by: (a) Gora, E. *Z. Phys.* **1942**, *120*, 121. (b) Feshbach, H. *Phys. Rev.* **1948**, *74*, 1548. (c) Sueoka, S. *J. Phys. Soc. Jpn.* **1949**, *4*, 361. (d) Lax, M. *Phys. Rev.* **1950**, *A79*, 200. (e) Pryce, M. H. L. *Proc. Phys. Soc. (London)* **1950**, *A63*, 25.

(39) (a) Löwdin, P.-O. *J. Chem. Phys.* **1951**, *19*, 1396. (b) Löwdin, P.-O. *J. Mol. Spectrosc.* **1963**, *10*, 12. (c) Löwdin, P.-O. *J. Mol. Spectrosc.* **1964**, *13*, 326. (d) Löwdin, P.-O. *J. Math. Phys.* **1962**, *3*, 969. (e) Löwdin, P.-O. *J. Mol. Spectrosc.* **1964**, *14*, 112.

(40) Löwdin, P.-O.; Pauncz, R.; de Heer, J. *J. Math. Phys.* **1960**, *1*, 461.

(41) Ziman, J. M. *Elements of Advanced Quantum Theory*; Cambridge University: Cambridge, 1969.

(42) Löwdin, P.-O. *J. Mol. Spectrosc.* **1964**, *14*, 119.

(43) (a) Smith, B. T.; Boyle, J. M.; Dongarra, J. J.; Garbow, B. S.; Ikebe, Y.; Klema, V. C.; Moler, C. B. *Matrix Eigensystem Routines—EISPACK Guide*; Springer-Verlag: Berlin, 1974. (b) Wilkinson, J. H.; Reinsch, C. *Handbook for Automatic Computation. Vol. II. Linear Algebra*; Springer-Verlag: Berlin, 1971. (c) Dongarra, J. J.; Moler, C. B.; Bunch, J. R.; Stewart, G. W. *LINPACK Users Guide*; Society for Industrial and Applied Mathematics: Philadelphia, 1979. (d) *IMSL Library Reference Manual*, 8th ed.; IMSL Inc.: Houston, 1980, Chapter L.

(44) (a) Wilkinson, J. H. *The Algebraic Eigenvalue Problem*; Oxford University: London, 1965. (b) Parlett, B. N. *The Symmetric Eigenvalue Problem*; Prentice-Hall: Englewood Cliffs, 1980.

(45) For a critical evaluation of diagonalization methods used in CI calculations, see: (a) Davidson, E. R. In *Methods in Computational Molecular Physics*; Diercksen, G. H. F., Wilson, S., Eds.; D. Reidel: Dordrecht, 1983; p 95. (b) Nesbet, R. K. In *Sparse Matrices and Their Uses*; Duff, I. S., Ed.; Academic: New York, 1981; p 161.

(46) (a) Fadeev, D. K.; Fadeeva, V. N. *Computational Methods of Linear Algebra*; W. H. Freeman and Company: San Francisco, 1963; Section 61. (b) Nesbet, R. K. *J. Chem. Phys.* **1965**, *43*, 311. (c) Shavitt, I. *J. Comp. Phys.* **1970**, *6*, 124. (d) Shavitt, I.; Bender, C. F.; Pipano, A.; Hosteny, R. P. *J. Comp. Phys.* **1973**, *11*, 90. (e) Raffenetti, R. C. *J. Comp. Phys.* **1979**, *32*, 403.

(47) Convergence difficulties with the relaxation method for near-degenerate eigenvalues are discussed in: (a) Davidson, E. R. *J. Comput. Phys.* **1975**, *17*, 87. (b) Reference 46c.

(48) (a) Ruhe, A. *Math. Comp.* **1974**, *28*, 695. (b) Ruhe, A. *J. Comp. Phys.* **1975**, *19*, 110. (c) Schwarz, H. R. *Comp. Meth. Appl. Mech. Eng.* **1974**, *3*, 11. (d) Schwarz, H. R. *Numer. Math.* **1974**, *23*, 135. (e) Ruhe, A. In *Sparse Matrix Techniques*; Barker, V. A., Ed.; Springer-Verlag: Berlin, 1977; p 130. (f) Nisbet, R. M. *J. Comp. Phys.* **1972**, *10*, 614. (g) Also: Nex, C. M. M. *J. Comp. Phys.* **1987**, *70*, 138.

rate of oscillation between eigenvalues but did not improve convergence.

An adequate alternative to the relaxation methods is an algorithm due to Davidson[45a,47a] that is a hybrid of direct methods and relaxation. Davidson's algorithm allows one to calculate not only the lowest few eigenvalues but also any eigenvalues within a selected energy range. The method is without the convergence difficulties associated with coordinate relaxation, yet still retains its conceptual simplicity and its transparent connection with perturbation theory.

Davidson's method can be used to find a selected eigenvalue and eigenvector by starting with a small subspace of the complete problem. The eigenvalues and eigenvectors of the small problem are calculated exactly by a standard matrix diagonalization routine and then coordinate relaxation is employed to expand the subspace by one vector. The added function is a combination of basis functions, with coefficients determined by perturbation theory. The new function is orthogonalized to each vector in the existing subspace and the larger problem is solved exactly. The process is continued until the desired eigenvalue and eigenvector are known to sufficient accuracy. In practice, very few iterations are required to ensure convergence if the dominant component of the eigenvector is contained in the initially chosen subspace. Thus, including in the subspace the crystal orbital that most closely approximates the desired MO ensures a rapidly convergent procedure. Subsequent eigenvalues and eigenvectors can be found quickly by using information provided by the diagonalization process required to find the first eigenvalue.

Numerical Results: Butadiene

A computer program was written to solve for cluster MO's using a crystal orbital basis set, combined with Davidson's algorithm. The program logic is displayed in Figure 2. First, crystal orbitals from a band calculation for a small unit cell were read and converted to crystal orbitals for the large unit cell corresponding to the cluster. Next, crystal orbitals were converted to Wannier functions. When the number of special k points used in the band calculation was exactly sufficient to give the correct number of Wannier functions, approximate Wannier functions were identical with the calculated crystal orbitals. The orbital phases were then adjusted so that the resulting orbitals were real and showed the symmetry of the large unit cell or cluster.[33c,49] After transforming the overlap and Hamiltonian matrices to the crystal orbital basis, the cluster orbitals and orbital energies were derived with Davidson's algorithm.

Davidson's algorithm was incorporated into the program with a matrix diagonalization subroutine based on published results,[50] but designed to optimize speed and flexibility for this particular problem. Thus, the program can find a specified set of eigenvalues and eigenvectors without solving for lower energy roots first. In addition, the program incorporates a root homing procedure[51] that guarantees convergence to the eigenvector having a selected crystal orbital as its dominant component. These options proved particularly powerful for deriving a small set of chemically relevant cluster orbitals. Cluster frontier orbitals, for example, could be calculated from crystal orbitals that appeared near the Fermi level in the band calculation. To achieve this capability, the initial subspace was formed of nonorthogonal crystal orbitals. Only the vectors subsequently added to the subspace were orthogonalized to the current orbital set in each iteration. The result was some increase in computation time because overlap had to be explicitly included in the calculation.

As a first test, the exact orbitals of butadiene were calculated from polyacetylene crystal orbitals and the orbitals of two capping hydrogens, making no approximations in the matrix diagonalization step. **9a–d** show the four polyacetylene orbitals taken to approximate the π orbitals of butadiene. The k values labeling the levels in **9** are analogous to those in **7**, but they refer to a unit cell containing two CH units (and are expressed in units of $2\pi/a$). The lowest level is the completely bonding combination of carbon p_z, formed from an orbital that is bonding within the unit cell and propagated to the next cell of the solid with approximately the same phase. If the k value associated with this orbital were $k = 0$, atomic orbital coefficients in neighboring cells would be exactly in-phase and **9a** would have a constant amplitude along the butadiene chain. The k value associated with this crystal orbital is not zero, but it is close ($k = 0.167$). As a result, orbitals in the two cells shown in **9a** still have the same phase, but unequal amplitudes appear along the chain. The k value thus serves to fix the nodal structure and, to some extent, tailor the orbital's behavior near the ends of the molecule.

The other levels in **9** can be understood in a similar way. The singly noded π orbital, for example, is also derived from the orbital that is bonding within the unit cell. Its k value ($k = 0.333$) is close to $k = 0.5$, where orbitals in neighboring cells would have exactly opposite phases, so it propagates with changing phase. The remaining two orbitals are descended from the orbital with π^* character within the unit cell, propagated with either the same phase ($k = 0.167$) or opposite phase ($k = 0.333$). The orbitals in **9** bear an obvious resemblance to the butadiene π levels, but they are not identical.

10 shows how the crystal orbitals of polyacetylene, **9**, mix to form the exact butadiene π levels. Since the butadiene molecule has a twofold rotation axis bisecting the middle carbon–carbon bond and perpendicular to the plane of the molecule, the four π levels shown in **9** can only mix in pairs. Furthermore, the capping

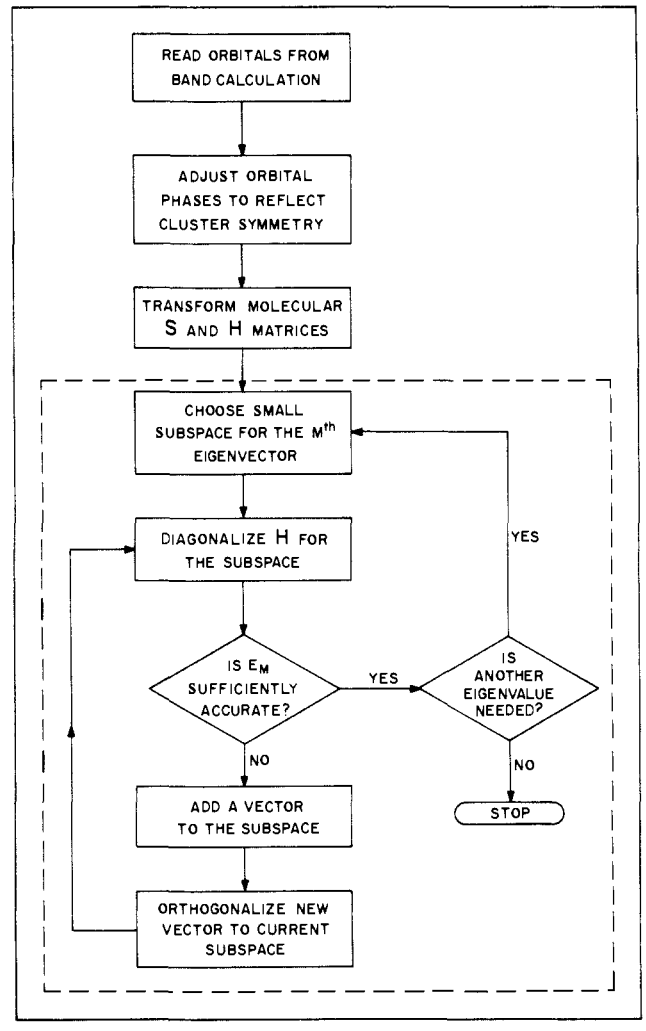

Figure 2. Flow diagram of program logic. Steps inside the dashed lines are part of the diagonalization routine based on Davidson's algorithm.

(49) (a) Krüger, E. *Phys. Status Solidi* **1972**, *B52*, 215, 519. (b) Kohn, W. *Phys. Rev.* **1973**, *B7*, 4388. (c) von Boehm, J.; Calais, J. L. *J. Phys.* **1979**, *C12*, 3661. (d) Zak, J. *Phys. Rev.* **1981**, *B23*, 1704; **1982**, *B26*, 3010.

(50) (a) Weber, J.; Lacroix, R.; Wanner, G. *Comput. Chem.* **1980**, *4*, 55. (b) Cisneros, G.; Bunge, C. F. *Comput. Chem.* **1984**, *8*, 157. (c) Cisneros, G.; Berrondo, M.; Bunge, C. F. *Comput. Chem.* **1986**, *10*, 281.

(51) Butscher, W.; Kammer, W. E. *J. Comput. Phys.* **1976**, *20*, 313.

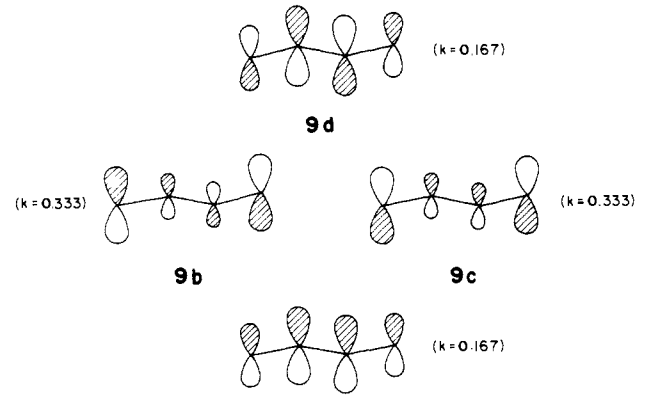

hydrogen orbitals are orthogonal to the π levels and do not mix in at all. **10a** illustrates how **9d** mixes slightly with **9a** to build up AO coefficients near the middle of the molecule to form the completely bonding MO. In a similar way, the other orbitals mix in pairs to give the other π MO's of butadiene. In each case, the crystal orbital goes over to the MO with a nodal pattern most like its own by mixing only a small amount of one other crystal orbital.

The crystal orbital approximation for the π levels of butadiene is, in fact, excellent. The lowest energy π level is 99% on the dominant crystal orbital, while the highest energy π level, with 95% of one crystal orbital, is the worst case. This simple example

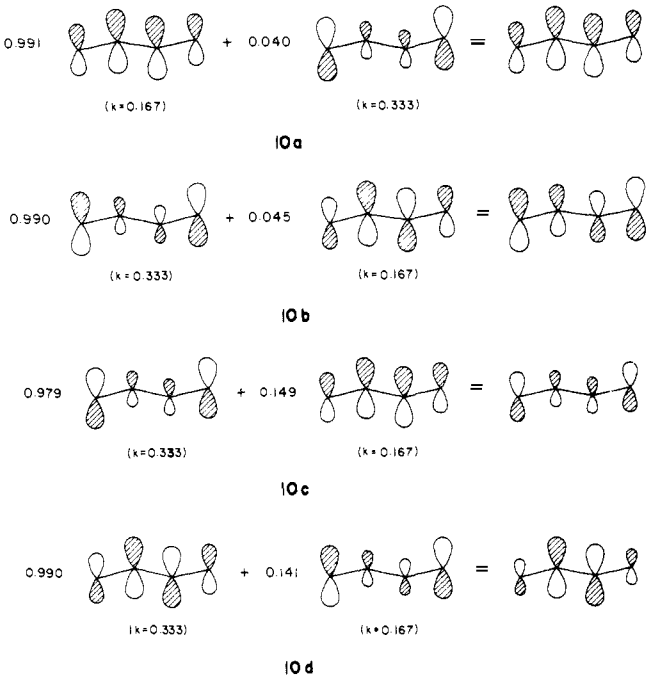

thus shows several important, general features associated with the derivation of cluster molecular orbitals from a band calculation. First, crystal orbitals with different k are orthogonal in the infinite solid but are allowed to mix once translational symmetry is destroyed. Second, the mixing occurs only to a very small extent, indicating that polyacetylene crystal orbitals are excellent approximate MO's, even for such a short chain as butadiene.

Since orbitals in the σ system of butadiene can mix strongly with orbitals on the end-capping hydrogens, approximating MO's as crystal orbitals is a more severe approximation for the σ system than for the π orbitals. Nonetheless, each of the bonding σ MO's is heavily concentrated in one crystal orbital. The lone exceptions are the two C–H σ bonding levels. We do not give the details here, but these two MO's are only 46% and 42% on their dominant crystal orbital. As the chain grows longer, the bonding crystal orbitals become still better approximate MO's. As expected, the molecular orbitals of the cluster approach the crystal orbitals of the solid as the cluster becomes larger. Further details for rhodium chains are presented in the following section.

Extensive testing was done to determine the minimum computation time needed to achieve acceptable eigenvalues and eigenvectors for the butadiene example, longer polyene chains, and rhodium oligomers, as well as for molybdate chains to be discussed in a separate paper.[14] For all test calculations, it was found that convergence was fastest if the initial subspace consisted of only the one or two dominant crystal orbital(s) and the orbitals on capping atoms. Orthogonalizing the added vectors to this nonorthogonal initial set, rather than using the other nonorthogonal crystal orbitals, speeds convergence. For example, the lowest MO of butadiene is calculated to within 10^{-4} eV of its exact value after only five iterations, using a starting set of three orbitals. The final subspace therefore consists of seven orbitals, or one-third of the 22 AO's in the original basis set. This represents a substantial savings over the time required to diagonalize the entire 22 × 22 matrix. A subspace of the same size, seven orbitals, is required to find the lowest eigenvalue and eigenvector of much longer polyene chains as well. These results, and the results for the rhodium oligomers described in the next section indicate that Davidson's algorithm provides an efficient way to find several selected eigenvalues and eigenvectors for large clusters, starting from the crystal orbitals for the related infinite solid.

The Rhodium Oligomers

Of the many known metal–metal bonded systems, the generic rhodium dimer shown in **11** is probably the best characterized. The molecule is the subject of innumerable synthetic, crystallographic, spectroscopic, and electrochemical studies.[13] It forms with a variety of bidentate ligands, L_2, and with two, one, or zero axial ligands. The rhodiums are square-planar coordinate and the bidentate nature of the bridging ligands forces the molecule into an eclipsed conformation. Usually each rhodium has a 2+

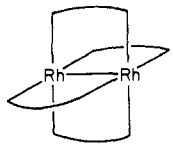

11

$Rh_2(L_2)_4^{n+}$

formal oxidation state, giving the dimer a total of 2(9 − 2) = 14 d electrons, a $\sigma^2\pi^4\delta^2\delta^{*2}\pi^{*4}$ electronic configuration, and a formal Rh–Rh single bond. Controversy regarding the bond order of the tetracarboxylate species prompted several detailed experimental[52] and theoretical[53] studies to verify this description of the Rh–Rh bond and to investigate the influence of varying the axial ligands.

The rhodium dimers are known to oligomerize in solution to form molecules with as many as 12 rhodiums.[54,55] **12** shows the X-ray structure of one such oligomer, $[Rh_2(CN(CH_2)_3NC)_4]_2Cl^{5+}$.[56] The molecule is a dimer of $[Rh_2(L_2)_4]$

(52) (a) Porai-Koshits, M. A.; Antsyshkina, A. S. *Dokl. Akad. Nauk SSSR* **1962**, *146*, 1102. (b) Cotton, F. A.; DeBoer, B. G.; LaPrade, M. D.; Pipal, J. R.; Ucko, J. *J. Am. Chem. Soc.* **1970**, *92*, 2926. *Acta Crystallogr.* **1971**, *B27*, 1664. (c) Martin, D. S., Jr.; Webb, T. R.; Robbins, G. A.; Fanwick, P. E. *Inorg. Chem.* **1979**, *18*, 475. (d) Cannon, R. D.; Powell, D. B.; Sarawek, K.; Stillman, J. S. *J. Chem. Soc., Chem. Commun.* **1976**, 31. (e) Moszner, M.; Ziolkowski, J. J. *Bull. Acad. Pol. Sci., Ser. Sci. Chim.* **1976**, *24*, 433. (f) Mulazzani, Q. G.; Emmi, S.; Hoffman, M. Z.; Venturi, M. *J. Am. Chem. Soc.* **1981**, *103*, 3362. (g) Wilson, C. R.; Taube, H. *Inorg. Chem.* **1975**, *14*, 405. (h) Kawamura, T.; Fukamachi, K.; Hayashida, S. *J. Chem. Soc., Chem. Commun.* **1979**, 945. (i) Kawamura, T.; Fukamachi, K.; Sowa, T.; Hayashida, S.; Yonezawa, T. *J. Am. Chem. Soc.* **1981**, *103*, 364.

(53) (a) Dubicki, L.; Martin, R. L. *Inorg. Chem.* **1970**, *9*, 673. (b) Norman, J. G., Jr.; Kolani, H. J. *J. Am. Chem. Soc.* **1978**, *100*, 791. (c) Bursten, B.; Cotton, F. A. *Inorg. Chem.* **1981**, *20*, 3042. (d) Nakatsuji, H.; Ushio, J.; Kanda, K.; Onishi, Y.; Kawamura, T.; Yonezawa, T. *Chem. Phys. Lett.* **1981**, *79*, 299. (e) Norman, J. G., Jr.; Renzoni, G. E.; Case, D. A. *J. Am. Chem. Soc.* **1979**, *101*, 5256.

(54) (a) Sigal, I. S.; Gray, H. B. *J. Am. Chem. Soc.* **1981**, *103*, 2220. (b) Sigal, I. S.; Mann, K. R.; Gray, H. B. *J. Am. Chem. Soc.* **1980**, *102*, 7252.

(55) (a) Balch, A. L. In *Extended Linear Chain Compounds*; Miller, J. S., Ed.; Plenum: New York, 1982; Vol. 1, p 1. (b) Albers, M. O.; Robinson, D. J. *Coord. Chem. Rev.* **1986**, *69*, 127.

fragments, with L = $CN(CH_2)_3NC$. Each Rh is square-planar

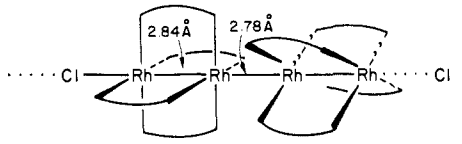

$[Rh_2(L_2)_4]_2Cl^{5+}$, $L_2 = CN(CH_2)_3NC$

12

coordinated by the CNR group of the bridging ligands. The bidentate bridges force an eclipsed conformation of ligands within each dimer, but between dimers the ligands prefer a staggered geometry. The central, unbridged Rh–Rh bond is shortest (2.78 Å), whereas the terminal metal–metal bonds are slightly longer (2.92 Å). Coordination of the terminal rhodiums is completed by a chloride ligand that is shared with neighboring molecules. If the bridging ligands are considered neutral and the chloride ligand has a 1– formal charge, six positive charges must be distributed over the four rhodiums. The result is two $Rh^{II}(d^7)$ and two $Rh^{I}(d^8)$ atoms and something less than four Rh–Rh single bonds. Electrochemical reduction of **12** gives a radical that oligomerizes further, to form Rh_8 and Rh_{12} chains.[54]

Platinum compounds related to the rhodium oligomers have also been structurally characterized. These molecules include an oligomer of four platinum atoms,[57] closely related to **12** and part of a larger class of compounds—platinum blues[58a,b]—important for their antitumor activity. Other related compounds are the infinite platinum chains such as the tetracyanoplatinates[58] shown in **13**. The tetracyanoplatinates are formed from aggregates of square-planar $Pt(CN)_4^{2-}$ molecules. Since each $Pt(CN)_4$ unit carries a 2– charge, each platinum is Pt^{II}, d^8. The square-planar

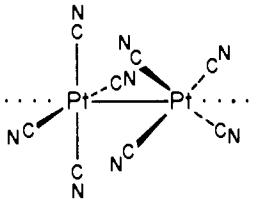

13

$_{\infty}^{1}[Pt(CN)_4^{2-}]$

fragments stack face-to-face, with ligands staggered, to give the infinite chains shown in **13**. Upon oxidation, Pt–Pt bonds strengthen and shorten.[58c,d]

The rhodium and platinum oligomers will be considered here as simple examples of transition-metal clusters cut from a one-dimensional solid. We begin with the infinite RhL_4 chain. A model $[RhH_4^{2-}]$ chain (with H^- ligands eclipsed) was used throughout and found to give no significant differences from the $[Rh(CNR)_4^{2+}]$ chain. In particular, the HOMO and LUMO for the model compound and for the experimentally characterized $[Rh_4(CNR)_{16}Cl]^{5+}$ molecule had identical Rh z^2 character, with the level above the LUMO more than 2 eV higher in every case.

Figure 3 shows selected energy bands of the model RhH_4^{2-} infinite chain. The lowest energy orbital at $k = 0$ is the completely in-phase, totally bonding combination of metal z^2. Next is the xy orbital with δ bonding character. Immediately above the δ level is a pair of degenerate π^* orbitals composed of rhodium xz and yz. Because the xz and yz orbitals have a nodal plane perpendicular to the chain and because orbitals propagate to the next cell with the same phase for $k = 0$, the π orbitals are antibonding at the zone center, $k = 0$. A second rhodium orbital of δ symmetry, $x^2 - y^2$, is strongly Rh–H σ antibonding and shows up too high in energy to appear in the figure.

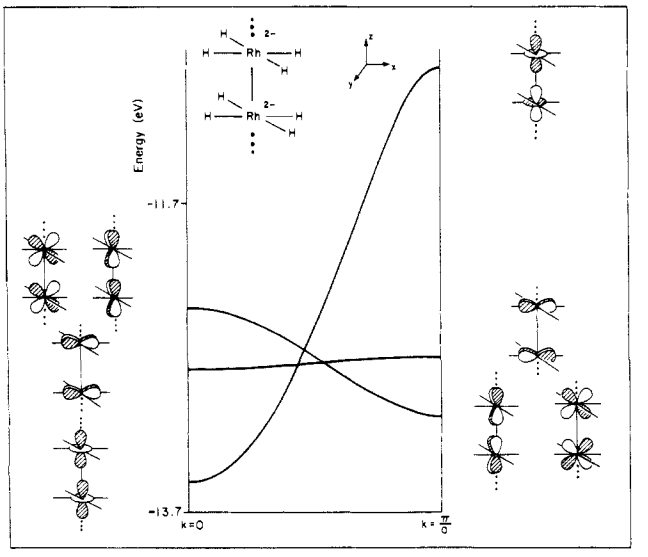

Figure 3. Metal d bands for the RhH_4^{2-} polymer.

The metal d orbitals show significant dispersion, or bandwidth, upon moving through the Brillouin zone. z^2 shows the largest dispersion because the σ overlap is greatest. Thus, the antibonding z^2 combination is the highest energy orbital at $k = \pi/a$. Since δ overlap is very small, the δ band shows small dispersion and is almost flat. The completely antibonding δ level is between the σ and π levels at $k = \pi/a$. The π levels have an overlap and therefore a dispersion that is intermediate between that of the σ and δ orbitals. At $k = \pi/a$, orbitals propagate with a change of phase, so the degenerate π levels are completely bonding at $k = \pi/a$.

The metal-based orbitals of an uncapped $[RhH_4]_4^{10-}$ oligomer are compared with the bands of the RhH_4^{2-} polymer in Figure 4. Oligomer σ orbitals are drawn out and all oligomer levels are labeled twice. One label refers to their symmetry in the D_{4h} point group; the second index describes their metal–metal bonding character. That second index labels the orbital according to its σ, π, or δ character along the chain and has a subscript indicating the number of nodes between atoms and perpendicular to the chain. Thus, the lowest energy level in the figure, σ_0, is the completely bonding combination of rhodium z^2 orbitals. σ_1 has one node perpendicular to the chain; σ_2 and σ_3 have two and three nodes, respectively. Like the σ band of the solid, σ orbitals of the oligomer show the largest dispersion among the metal d orbitals: σ_0 is the lowest energy metal level and σ_2 and σ_3 are the highest levels not involved in Rh–H bonding. The π levels split in a similar way. They are interspersed among the σ levels and have π_1 below π_2, with π_3 highest in energy. The δ orbitals hardly split at all. They have a "bandwidth" of only 0.08 eV and always remain filled for the usual electron counts.

The oligomer MO's displayed on the right of Figure 4 were calculated from crystal orbitals of the infinite chain. The band calculation was performed at a set of k points identical with the ones in **2** and **7** and described earlier. The calculation was also done using the special k point set from **8**, with only slightly different results. The simpler pattern of AO coefficients and strong connection with simple Hückel theory prompted us to present results for the points 0.1–0.4 (units of $2\pi/a$) marked at the bottom of the band structure in Figure 4. Circles on the various energy bands are marked by dots or crosses and appear at the k points marked at the bottom. The circles mark dominant crystal orbitals in the MO corresponding to the attached symmetry label.

Several important features of the LCCO method are contained in Figure 4. First, each MO corresponds to only one point on the

(56) Mann, K. R.; DiPierro, M. J.; Gill, T. P. *J. Am. Chem. Soc.* **1980**, *102*, 3965.
(57) Ginsberg, A. P.; O'Halloran, T. V.; Fanwick, P. E.; Hollis, L. S.; Lippard, S. J. *J. Am. Chem. Soc.* **1984**, *106*, 5430.
(58) (a) Wollins, J. D.; Kelly, P. F. *Coord. Chem. Rev.* **1985**, *65*, 115. (b) Lippard, S. J. *Science* **1982**, *218*, 1075. (c) Williams, J. M.; Schultz, A. J.; Underhill, A. E.; Carneiro, K. In *Extended Linear Chain Compounds*; Miller, J. S., Ed.; Plenum: New York, 1982; Vol. 1, p 73. (d) Holzapfel, W.; Yersin, H.; Gliemann, G. *Z. Kristallogr.* **1981**, *157*, 47.

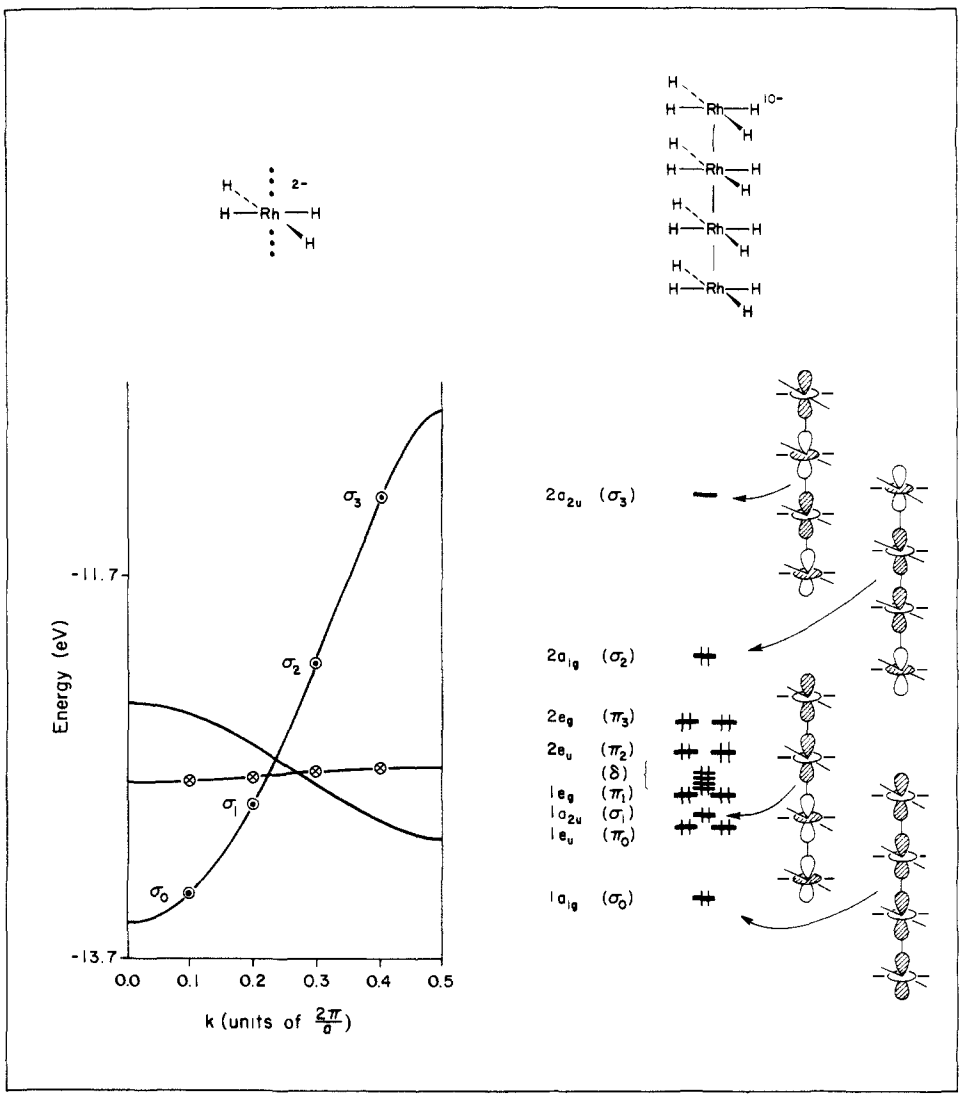

Figure 4. Metal-based MO's of the $[RhH_4]_4^{10-}$ oligomer (right) are derived from the polymer band calculation (left). MO's are labeled according to their symmetry in D_{4h} and their Rh–Rh bonding character. σ and δ crystal orbitals at chosen k points are marked according to their corresponding MO's for the finite chain.

band structure, indicating that each MO is made primarily from one crystal orbital. Second, the energy ordering of MO's and their dominant crystal orbitals is identical. This is a reflection of the similar AO composition and nodal structure of oligomer MO's and polymer crystal orbitals. The crosses mark crystal orbitals that are identical to oligomer MO's. They appear in the band formed from the *xy* orbitals and reflect the tiny magnitude of the δ overlap: since crystal orbitals at the chosen k points are the same as MO's only within the simple Hückel approximation, next-nearest-neighbor and more distant interactions between δ orbitals are essentially zero. Although the σ and π crystal orbitals are generally not identical with the oligomer MO's, they are a good approximation in every case. The σ MO's—σ_0 (composed 100% of its dominant crystal orbital), σ_1 (97.7%), σ_2 (99.6%), and σ_3 (98.2%)—are particularly close to their dominant crystal orbitals. In general, the polymer crystal orbitals for this simple case are excellent approximate MO's for the uncapped oligomer. Crystal orbitals have similar AO compositions, nodal structures, and energies as the corresponding molecular orbitals.

Capping the $[RhH_4]_4^{10-}$ oligomer with two Cl^- ligands to model the crystal field about the Rh in $[Rh_2(CN(CH_2)_3NC)_4]_2Cl^{5+}$, as shown in Figure 5, affects primarily the σ levels of the oligomer. Oligomer π levels rise very slightly in energy, whereas the δ orbitals are unperturbed because the capping ligands carry no orbitals of the right symmetry to interact. Interaction with the Cl^- σ orbitals pushes σ_0, σ_2, and σ_3 to higher energy without changing level orderings; σ_1, on the other hand, is pushed above the δ orbitals and several of the π's. σ_2 remains the HOMO and the completely antibonding σ_3 is the LUMO. This level ordering, as well as the substantial energy gap below the HOMO, is consistent with spectroscopic data and the ease of oxidation and reduction of the $[Rh_4(CN(CH_2)_3NC)_8]^{6+}$ molecule.[54,59] An additional, extremely important effect of adding capping ligands is the enhanced mixing between σ levels of the uncapped oligomer. The mixing between the occupied σ_1 and empty σ_3 is particularly important in determining metal–metal bond lengths.

Table I. Total Rh–Rh Overlap Populations, Rh–Rh Overlap Populations for the σ_1 Level, and Composition of σ_1 for Different Halide Ligands

	overlap populations		
	X = F	X = Cl	X = I
outer Rh–Rh bond	0.114	0.119	0.115
central Rh–Rh bond	0.127	0.117	0.099
outer Rh–Rh bond (σ_1)	0.098	0.102	0.094
central Rh–Rh bond (σ_1)	−0.034	−0.045	−0.065
$\sigma_1^c(F_2) = 95.8\%\ \sigma_1 + 2.5\%\ \sigma_3$			
$\sigma_1^c(Cl_2) = 85.5\%\ \sigma_1 + 8.1\%\ \sigma_3$			
$\sigma_1^c(I_2) = 49.1\%\ \sigma_1 + 28.9\%\ \sigma_3$			

The importance of ligand-induced mixing of the σ levels for $[Rh_4H_{16}X_2]^{12-}$ is shown by varying the capping ligand X. Table I displays the effect explicitly. Overlap populations, a measure of bond order, are approximately constant between end rhodiums

(59) Miskowski, V. M.; Gray, H. B. *Inorg. Chem.* **1987**, *26*, 1108.

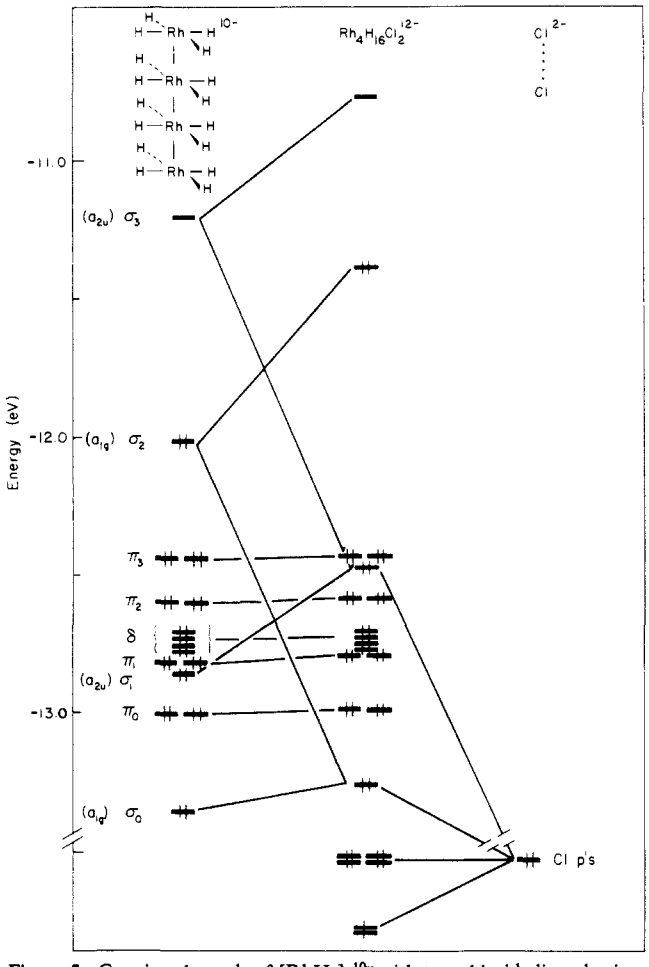

Figure 5. Capping the ends of $[RhH_4]_4^{10-}$ with two chloride ligands gives the energy levels of $[Rh_4H_{16}Cl_2]^{12-}$.

as the capping halide ligand is changed from fluoride to chloride to iodide. The central Rh–Rh bond, on the other hand, is progressively weakened. The bond weakening can be traced to the different character of the σ_1 level in each case. First, the contribution of the σ_1 orbital to metal–metal overlap populations is given in Table I to show that it takes on a more antibonding character (becomes more negative) between the central rhodiums as the capping ligands become less electronegative. In each case, the difference in overlap populations between central rhodiums due to the σ_1 level is approximately the same as the difference in total overlap population.

The different overlap populations can be traced to the different compositions of the σ_1 orbitals. As the capping ligands become less electronegative, the halogen levels move to higher energy, closer to the metal levels. Consequently, halogen orbitals mix more strongly with the lower energy metal levels and push them higher in energy. As a result, the σ_1 orbital mixes more with the σ_3 level of the uncapped oligomer. The mixing is indicated at the bottom of Table I, with orbital labels that were explained previously (the superscript "c" indicates a halide capped chain; no superscript implies an uncapped oligomer). Whereas the σ_1^c orbital for the fluoride chain contains only 2.5% of the σ_3 oligomer orbital, the iodide σ_1^c has a much larger 28.9% contribution from σ_3. Since σ_3 is more heavily concentrated on the central rhodiums than σ_1 and is noded between them, the result of the increased mixing is to enhance the antibonding interaction between central rhodiums of the σ_1^c orbital for the halide capped chains. This ligand-induced mixing between σ_1 and σ_3 depends on the electronegativity of the end-capping ligands and provides the opportunity to tune, experimentally, the central Rh–Rh bond length by varying the capping ligand.

The preceding analysis shows that oligomer end effects can be minimized by choosing the appropriate capping ligand. If end effects are neglected for the moment, several general conclusions regarding rhodium oligomers of varying lengths may be drawn from the band structure for the infinite polymer. As the oligomer becomes longer, its energy levels will begin to resemble the polymer band structure. k points where crystal orbitals resemble MO's of the finite chain will divide the band structure into smaller pieces and molecular orbital energies will move closer together. Energies of the most bonding and most antibonding MO's will move toward opposite ends of the k axis. In particular, the top of the z^2 band puts an upper limit on oligomer z^2 orbital energies. For high d electron counts (all metals d^7–d^8), the HOMO for arbitrarily large oligomers must therefore have metal z^2 character and must lie within the energy range spanned by the polymer z^2 band. The HOMO could abruptly change its AO composition with increasing chain length only if a higher energy band crossed the z^2 band at some point in the Brillouin zone.

The rhodium chain example also shows that preferred cluster electron counts will be found by considering not only band gaps for the infinite solid but also regions where there are few, steep bands and a low density of states.

Summary

A method has been developed to derive the orbitals of large clusters efficiently from the results of a band calculation. The results rest on two ideas: the reciprocal space of finite crystals and the expression of cluster MO's as linear combinations of crystal orbitals (LCCO's). The method has been tested and used to describe metal–metal bonding in experimentally characterized, short-chain rhodium oligomers. The connection between oligomer MO's and polymer crystal orbitals allows the results to be extrapolated with some confidence to finite rhodium chains of arbitrary length.

First, the reciprocal space of finite crystals is introduced and its relationship with the reciprocal lattice of the infinite crystal is explored. The one-to-one correspondence between k values in the two reciprocal spaces guides the choice of k points for a band calculation where crystal orbitals have a nodal structure that matches the nodes of cluster MO's. The relevant orbitals from the solid-state calculation are the familiar Wannier functions for a large unit cell corresponding to the cluster. Wannier functions can be derived from a band calculation for a smaller unit cell at one k point or at a selected set of special k points.

The orbitals from the band calculation are used in a computer program written to calculate selected cluster orbitals as linear combinations of crystal orbitals (LCCO's). The program employs an approximate matrix diagonalization routine based on an algorithm of Davidson's, originally used to solve the CI problem for small molecules. Approximations involve choosing a small subspace of the larger problem and solving for the eigenvalues and eigenvectors exactly within the chosen space. The close relationship to Brillouin–Wigner perturbation theory and a connection with the more common Green's function techniques is pointed out.

The method's performance was tested on long-chain, hydrocarbon polyenes and on transition-metal chains related to the known $[Rh_4(CN(CH_2)_3NC)_8Cl]^{5+}$ molecule. The method is capable of giving orbitals localized near the edges of the cluster as well as more delocalized levels. The delocalized levels are more concentrated in the orbitals of the solid and require slightly less computational effort. As the cluster or chain gets larger, the orbitals of the solid become better approximations to cluster MO's. Orbital energies for the cluster can be calculated to within 10^{-4} eV of their exact values with use of a subspace consisting of orbitals on edge-capping atoms plus only five to ten orbitals from the band calculation.

Although the method is illustrated with extended-Hückel calculations for large clusters, the approach is general and can be used in conjunction with any calculation method that gives crystal orbitals for the infinite solid. The current presentation emphasizes large, finite systems such as clusters or thin films, but the LCCO approach is equally valid for other systems perturbed from perfect translational periodicity. Examples include infinite

Table II. Parameters Used in the Extended-Hückel Calculations

	orbital	H_{ii} (eV)	ζ_1 (C_1[a])	ζ_2 (C_2[a])
Rh	4d	-12.73	5.54 (0.5563)	2.40 (0.6119)
	5s	-9.01	2.135	
	5p	-4.53	2.099	
I	5s	-18.0	2.68	
	5p	-12.7	2.32	
Cl	3s	-30.0	2.033	
	3p	-15.0	2.033	
F	2s	-40.0	2.425	
	2p	-18.1	2.425	
H	1s	-13.6	1.3	
C	2s	-21.4	1.625	
	2p	-11.4	1.625	

[a] Coefficients in the double-ζ d orbital expansion.

or semi-infinite systems such as surfaces, interfaces, and defects.

Conclusions for the rhodium chains are the following: (1) The length of the central Rh-Rh bond can be tuned by adjusting the electronegativity of the end-capping ligands. Highly electronegative caps such as fluoride give a short bond; less electronegative capping ligands such as iodide give a longer bond and nearly equal Rh-Rh bond lengths along the chain. The effect can be described as a ligand-induced mixing of MO's from the uncapped oligomer or of crystal orbitals from the infinite polymer. (2) For longer chains and high d electron counts (all rhodiums d^7-d^8), the HOMO must have Rh z^2 character and appear at an energy within the z^2 band of the infinite polymer. The HOMO-LUMO gap will smoothly decrease with increasing chain length. (3) Preferred cluster electron counts can be found by looking for low densities of states in the corresponding infinite solid. For the known molecule $[Rh_4(CN(CH_2)_3NC)_8Cl]^{5+}$, and for longer oligomers, they appear within the steep z^2 band of the infinite polymer—at electron counts near d^7-d^8.

Acknowledgment. We are grateful to Boon Teo for the inspiration to attack this problem and to H. A. Scheraga, who provided the support for L.P.'s stay in the United States. In addition, R.W. thanks Susan A. Jansen for helpful discussions and moral support, Peter P. Edwards and John Boland for useful suggestions regarding possible applications, and the Cornell University Materials Science Center and the NSF for support (Grant DMR 87422702).

Appendix

All calculations were performed with orbital exponents and Coulomb integrals taken from previous work[60] and listed in Table II. Idealized polyene geometries had C-C bond lengths of 1.4 Å, C-H bond lengths of 1.1 Å, and all angles of 120°. Rhodium-rhodium distances of 2.85 Å were taken to approximate Rh-Rh single bonds.[61] Rhodium-hydrogen (1.65 Å), Rh-Cl (2.63 Å), and Rh-I (2.76 Å) bond lengths were taken from published crystal structures.[56,62] Rh-F bond distances were estimated from the Rh-Cl distance and covalent radii (qualitative conclusions are valid over a range of Rh-X bond lengths of at least 0.5 Å). Idealized Rh coordination geometries were used so that all bond angles were 90° or 180°.

(60) (a) Hoffmann, R.; Minot, C.; Gray, H. B. *J. Am. Chem. Soc.* **1984**, *106*, 2001. (b) Canadell, E.; Eisenstein, O. *Inorg. Chem.* **1983**, *22*, 2398. (c) Summerville, R. H.; Hoffmann, R. *J. Am. Chem. Soc.* **1976**, *98*, 7240. (d) Andersen, A. B.; Hoffmann, R. *J. Chem. Phys.* **1974**, *60*, 4271.
(61) Mann, K. R.; Bell, R. A.; Gray, H. B. *Inorg. Chem.* **1979**, *18*, 2671.
(62) Balch, A. L.; Olmstead, M. M. *J. Am. Chem. Soc.* **1979**, *101*, 3128.

Trans-Edge-Sharing Molybdenum Octahedra: A Reciprocal Space Approach to Metal-Metal Bonding in Finite Chains[1]

Ralph A. Wheeler*,† and Roald Hoffmann*

Contribution from the Department of Chemistry and Materials Science Center, Cornell University, Ithaca, New York 14853. *Received January 25, 1988*

Abstract: Metal-metal bond lengths alternate at the apices of trans-edge-sharing octahedra in $In_{11}Mo_{40}O_{62}$. The bond alternation is a consequence of finite chain length: it is absent in $NaMo_4O_6$, the analogous infinite chain with a similar electron count. We trace the observed distortion to a set of σ levels with x^2-y^2 character and a nodal structure similar to the π levels of hydrocarbon polyenes. The apical pairing distortion mixes these levels with orbitals on basal molybdenums and enhances metal-metal bonding perpendicular to the chain, especially at the ends of the molecules. A second distortion involving octahedral tilting is found equally favorable for chains with an odd number of octahedra and a new charge partitioning between the clusters of $In_{11}Mo_{40}O_{62}$ is suggested. A newly developed linear combination of crystal orbitals (LCCO) method aids in comparing orbitals of the finite and infinite chains.

Solid-state chemistry is a burgeoning field, with new compounds and concepts being discovered almost daily. Unusual structures beget novel properties; fascinating new behavior fuels the search for still more compounds. From the synergism between chemistry and physics, patterns are beginning to develop. An understanding of solid-state structures and properties is emerging.

One key, unifying concept for materials chemistry and physics is the question of dimensionality. Extended, three-dimensional structures are often discussed in terms of smaller units such as layers,[2] chains,[3] or clusters,[4] but one may question the validity of such a picture. Are the fragments that make up the solid weakly coupled, or is the compound actually three-dimensional? A chemical approach to this puzzle involves searching for chemical

† Current address: Department of Chemistry, University of Houston; Houston, TX 77204-5641.

(1) Based on: Wheeler, R. A. Ph.D. Thesis, Cornell University, October, 1987; Chapter III.

(2) (a) O'Keeffe, M.; Hyde, B. G. *Philos. Mag.* **1980**, *295A*, 38. (b) Hulliger, F. *Structural Chemistry of Layer-Type Phases*; D. Reidel: Dordrecht, 1976. (c) Pearson, W. B. *The Crystal Chemistry and Physics of Metals and Alloys*; Wiley-Interscience: New York, 1972.

(3) (a) *Crystal Chemistry and Properties of Materials with Quasi-One-Dimensional Structures*; Rouxel, J., Ed.; D Reidel: Dordrecht, 1986. (b) *Electronic Properties of Inorganic Quasi-One-Dimensional Compounds*; Monceau, P., Ed.; D. Reidel: Dordrecht, 1985; Vol. I-II. (c) *Extended Linear Chain Compounds*; Miller, J. S., Ed.; Plenum: New York, 1982; Vol. 1-3. (d) *Highly Conducting One-Dimensional Solids*; Devreese, J. T., Evrard, R. P., Van Doren, V. E., Eds.; Plenum: New York, 1979.

0002-7863/88/1510-7315$01.50/0